

Observing Rotation-powered Pulsars and Magnetars in the X-ray and Gamma-Ray Sky

**Wim Hermsen
SRON Netherlands Institute for Space Research, Utrecht
&
Astronomical Institute Anton Pannekoek, Univ. of Amsterdam**

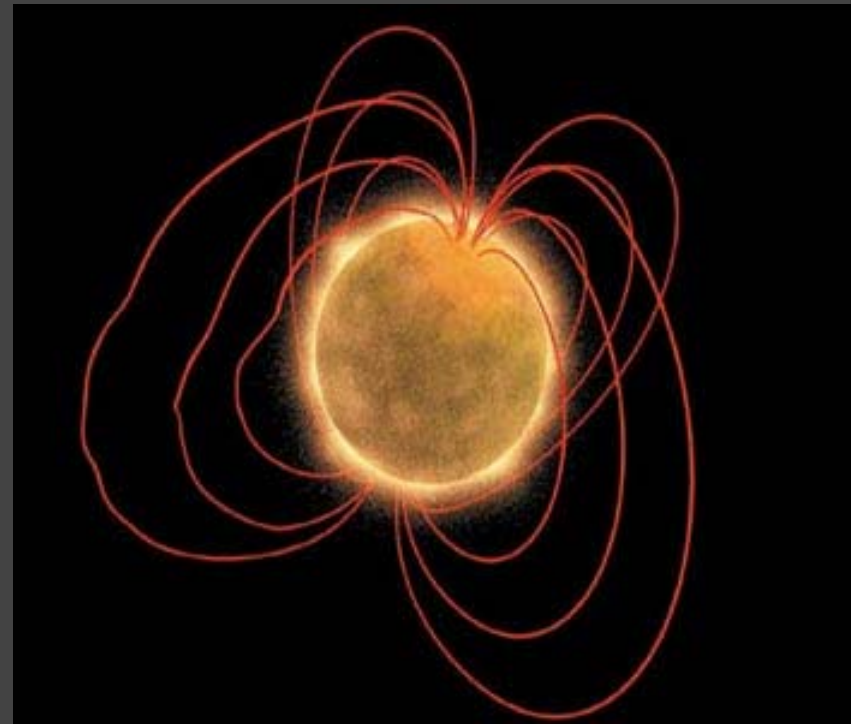
Cargese, 13-14 April 2006

Observing Rotation-powered Pulsars and Magnetars in the X-ray and Gamma-Ray Sky

PART 1

- Population of Rotation-powered Pulsars and Magnetars
- Rotation-Powered Pulsars
 - Status and Recent X-ray and Gamma-Ray Observations:
Normal and millisecond pulsars
 - Review Emission Models, Comparison with
Observations

Population of Rotation-powered Pulsars and Magnetars



Rotating Neutron Stars

- **Rotation-powered pulsars (mostly Radio Pulsars):**

$$L_{\text{tot(EB)}} < E_{\text{spin-down}} = \dot{E} \sim 10^{34-38} \text{ erg s}^{-1}$$

- **Magnetars:**
 - Soft Gamma-Ray Repeaters (SGRs)**
 - Anomalous X-ray Pulsars (AXPs)**

$$L_{\text{tot(EB)}} \gg E_{\text{spin-down}} \sim 10^{33} \text{ erg s}^{-1}$$

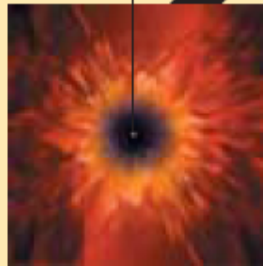
L_x up to $\sim 10^{36} \text{ erg s}^{-1}$ (0.2 – 10 keV)

$L_{x/\gamma}$ up to $\sim 10^{44} \text{ erg s}^{-1}$ in peak of giant SGR outburst

TWO TYPES OF NEUTRON STARS

1 Most neutron stars are thought to begin as massive but otherwise ordinary stars, between eight and 20 times as heavy as the sun.

2 Massive stars die in a type II supernova explosion, as the stellar core implodes into a dense ball of subatomic particles.

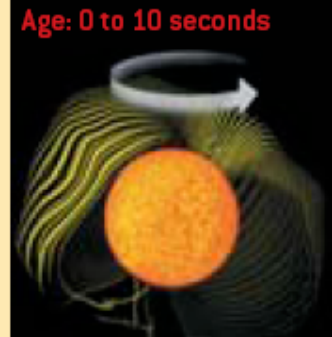


NEWBORN NEUTRON STAR

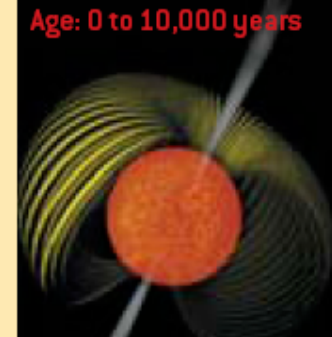
MAGNETAR

ORDINARY PULSAR

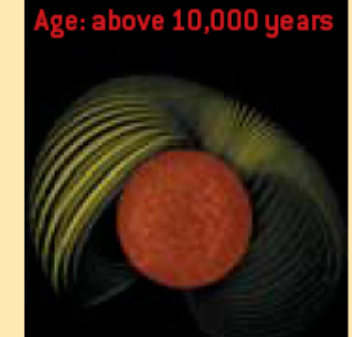
3A: If the newborn neutron star spins fast enough, it generates an intense magnetic field. Field lines inside the star get twisted.



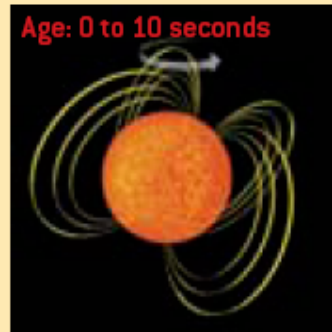
4A: The magnetar settles into neat layers, with twisted field lines inside and smooth lines outside. It might emit a narrow radio beam.



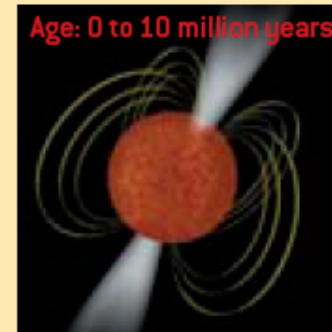
5A: The old magnetar has cooled off, and much of its magnetism has decayed away. It emits very little energy.



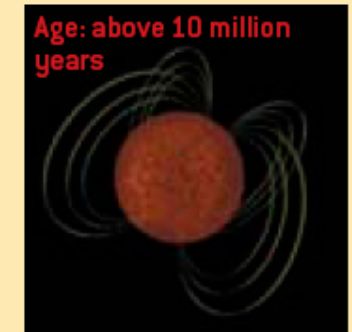
3B: If the newborn neutron star spins slowly, its magnetic field, though strong by everyday standards, does not reach magnetar levels.



4B: The mature pulsar is cooler than a magnetar of equal age. It emits a broad radio beam, which radio telescopes can readily detect.



5B: The old pulsar has cooled off and no longer emits a radio beam.



Rotation-Powered Pulsars and Magnetars

| | RP Pulsars | Magnetars |
|--------------|---------------------------------------|-------------------------|
| Similarities | Spinning-down neutron stars | |
| | $P \sim 1.5 \text{ ms} - 8 \text{ s}$ | $P \sim 5-11 \text{ s}$ |
| | Pulsed high-energy emission | |
| | Particle acceleration | |
| | Glitches | |
| Differences | No bursts | Bursts |
| | Weak X-ray for same P s | Strong X-ray |
| | Radio | No radio |
| | Rotation power | Magnetic power |

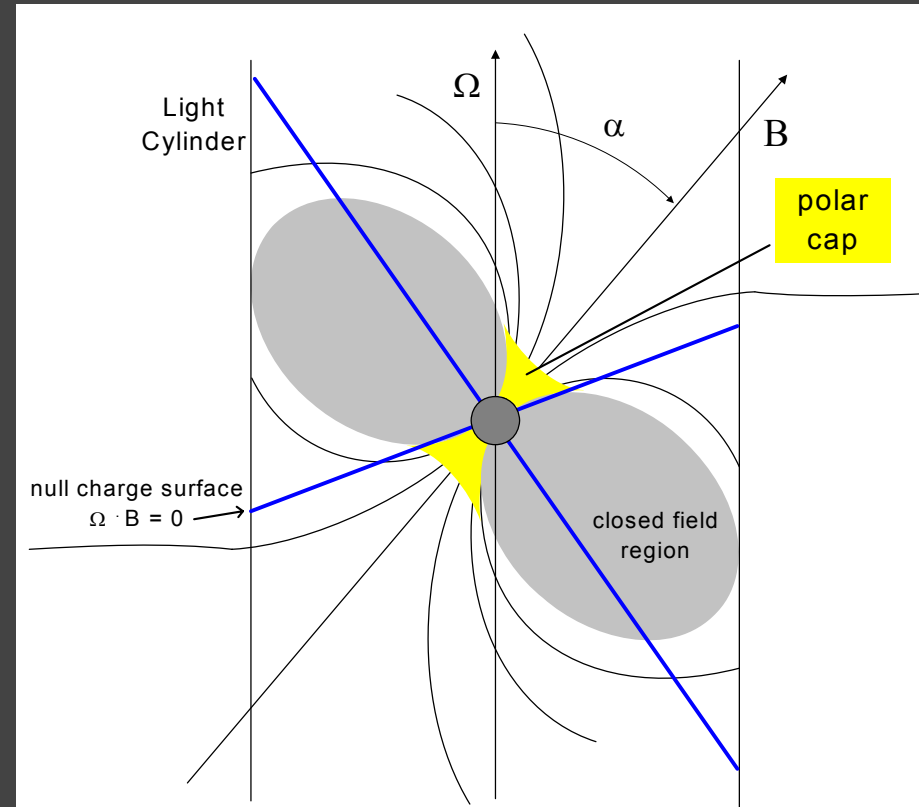
Pulsar Characteristic Parameters

- Period P
- Period derivative \dot{P}
- Rotational energy loss $\dot{E} = I\Omega\dot{\Omega}$
 I moment of inertia, $\Omega = 2\pi/P$
- Spin-down flux $F = \dot{E} / 4\pi d^2$
 d distance
- Characteristic age $\tau_c = P / 2\dot{P}$
- Open field line voltage

$$V_{PC} = 4 \times 10^{20} P^{-3/2} \dot{P}^{1/2} \text{ V}$$

- Averaged magnetic field strength at neutron star surface

$$B_s = 3.3 \times 10^{19} (P\dot{P})^{1/2} \text{ (assuming simple magnetic dipole braking in vacuum)}$$



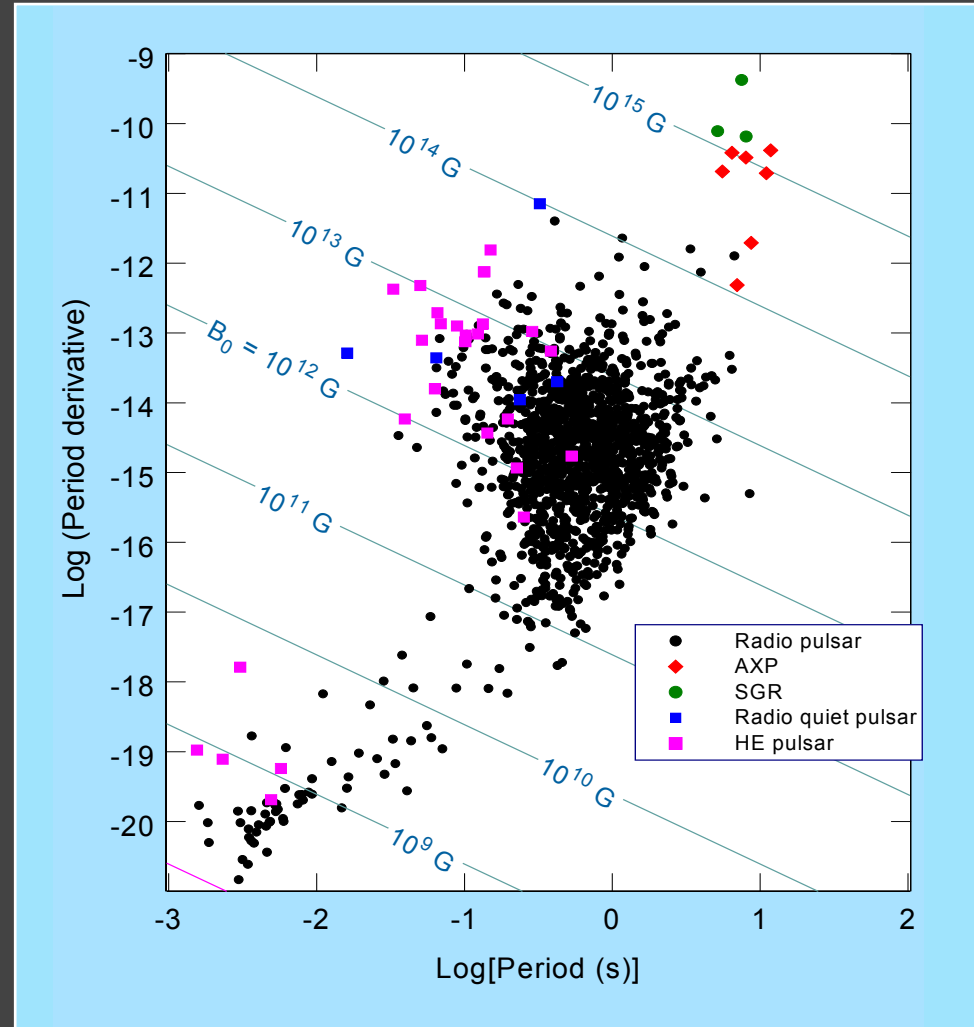
Rotation-Powered Pulsars and Magnetars:

P- \dot{P} diagram with $B_0 = B_s$

- ~ 1500 radio pulsars
- ~ 30 X-ray pulsars
- 10 γ -ray pulsars
- 7 AXPs
- 5 SGRs

Extreme B fields:

- AXPs & SGRs $10^{14} - 10^{15}$ G
- Millisecond pulsars $10^8 - 10^{10}$ G (old "recycled" pulsars, spun-up by accretion torques in a binary system)

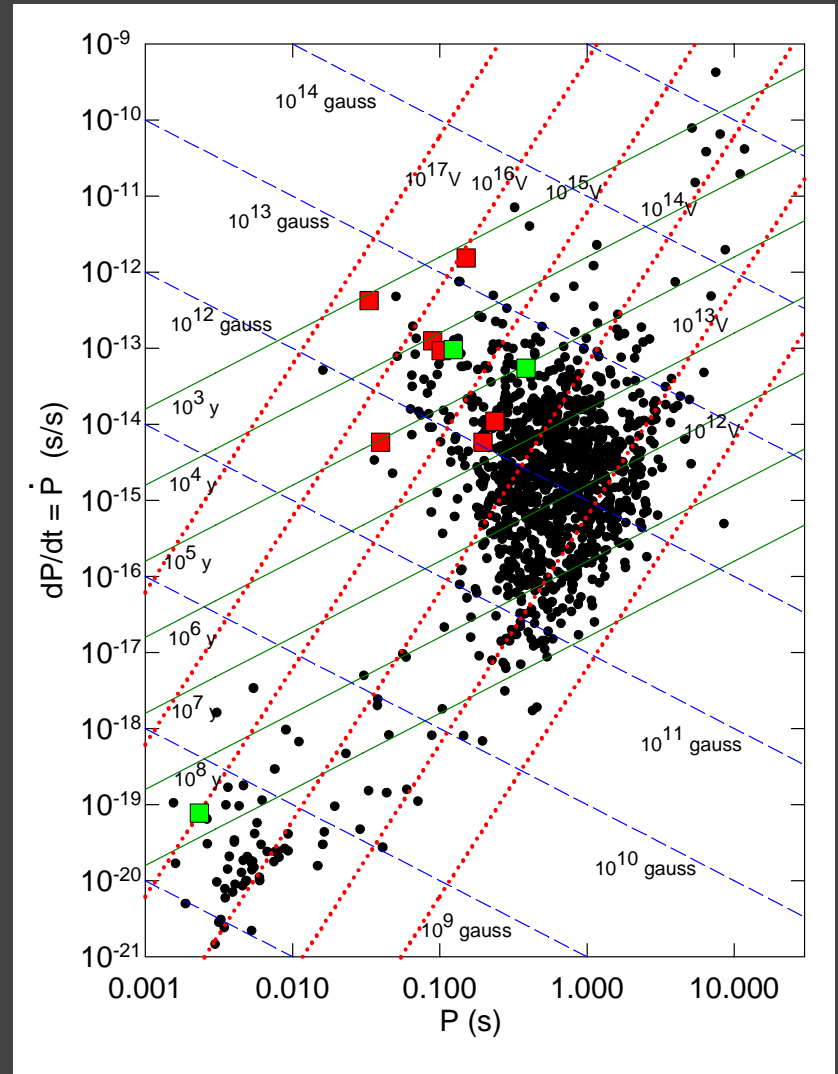


Rotation-Powered Pulsars and Magnetars:

P- \dot{P} diagram with B_S , τ_C , V_{PC}

  } High-confidence & lower-confidence detections of high-energy (>100 MeV) gamma-ray pulsars

Millisecond pulsar
PSR J0218+4232

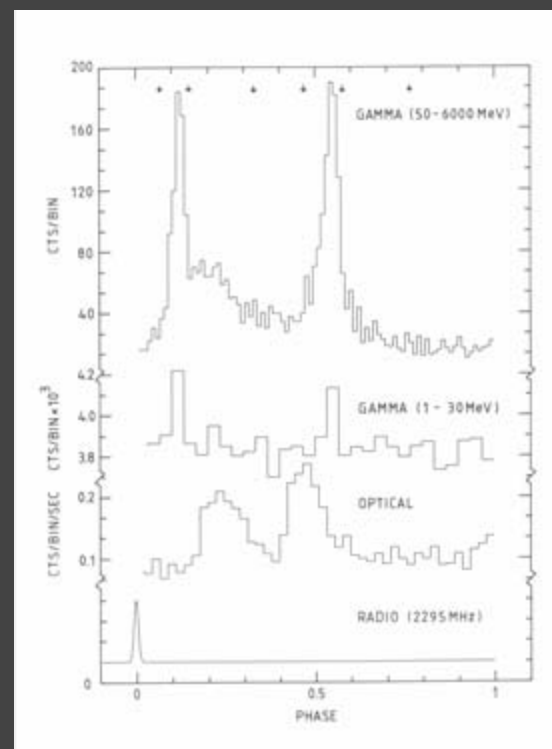
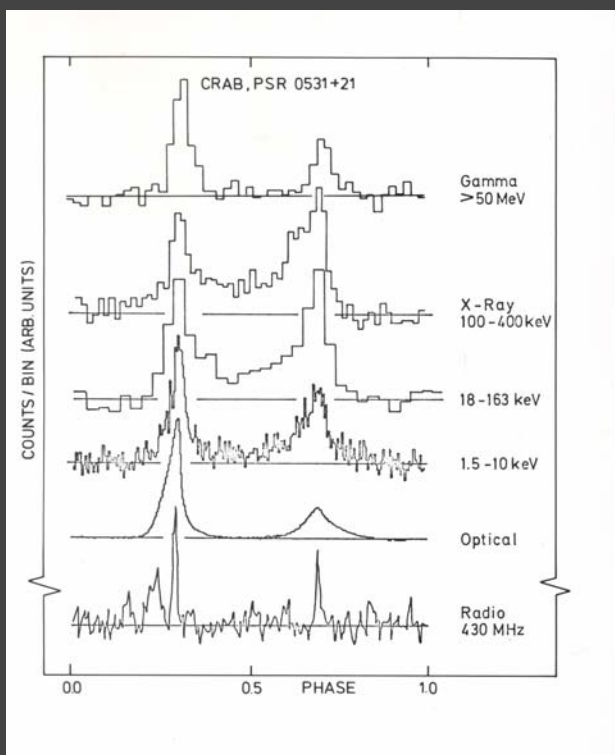


Rotation-Powered Pulsars

- Status and Recent X-ray and Gamma-Ray Observations:

Normal and millisecond pulsars

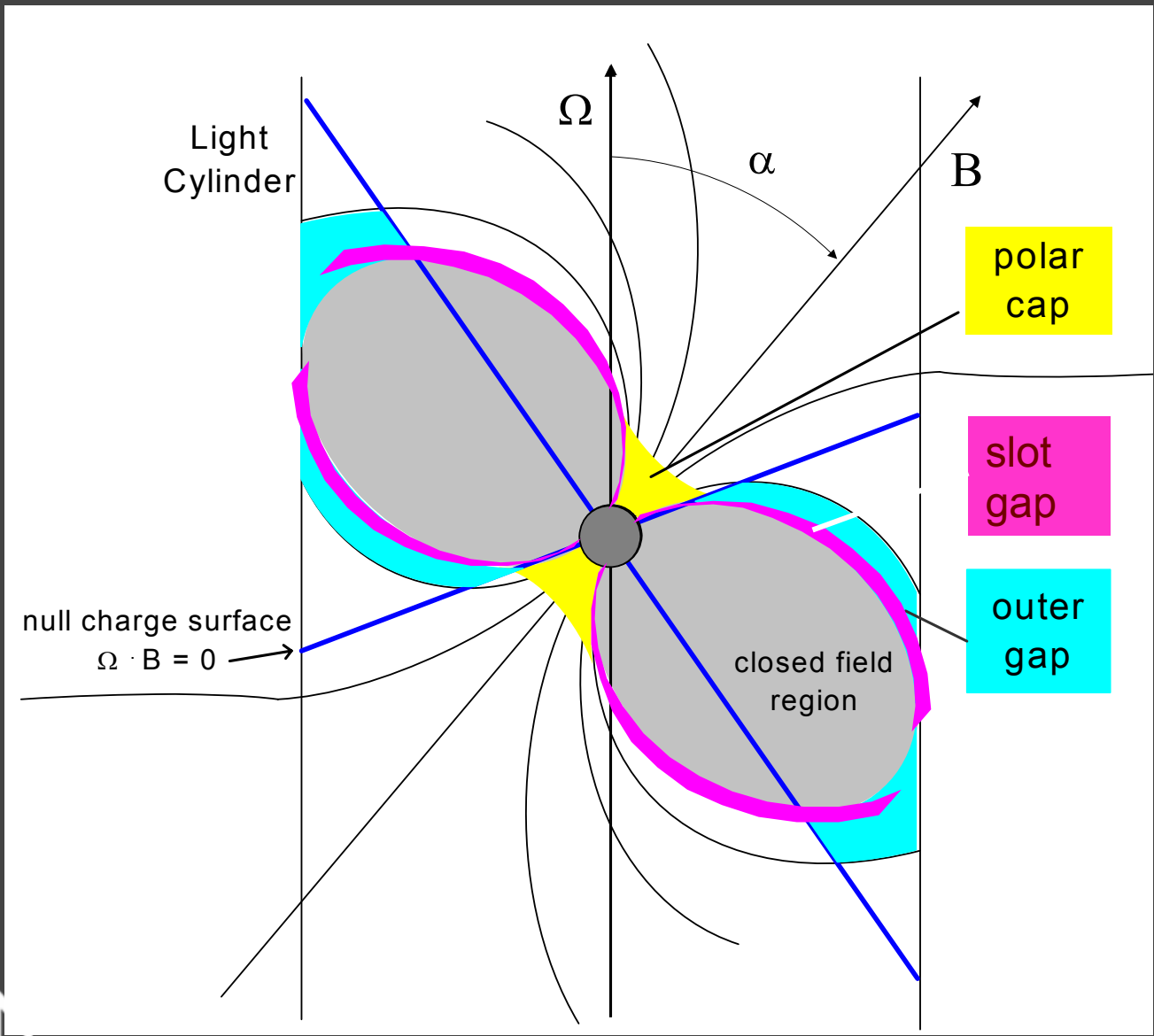
Crab and Vela profiles: Gamma rays (COS-B) down to the radio ≥ 25 years ago !



For 30 years Polar Cap models v.s. Outer Gap models !

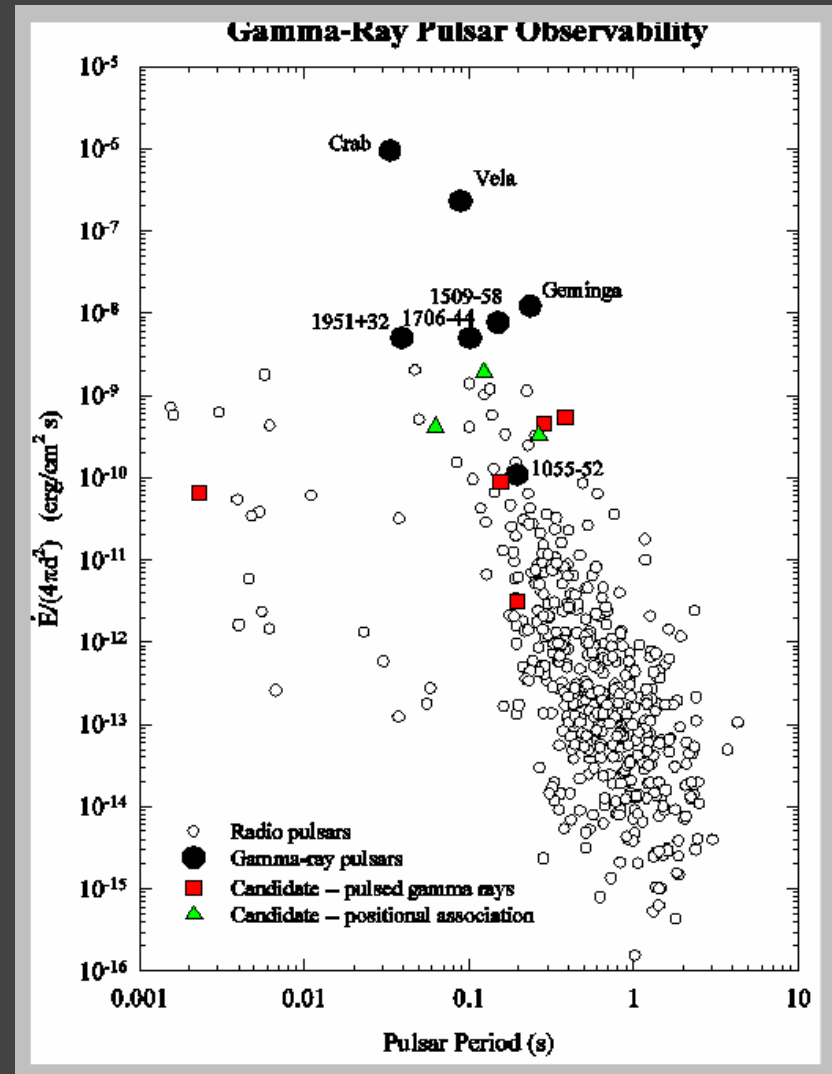
Progress in our understanding of the production of non-thermal X-ray and gamma-ray emission in pulsar magnetospheres has been slow. Particularly, because of the slow advance made in the observations.

Geometries of high-energy emission pulsar models



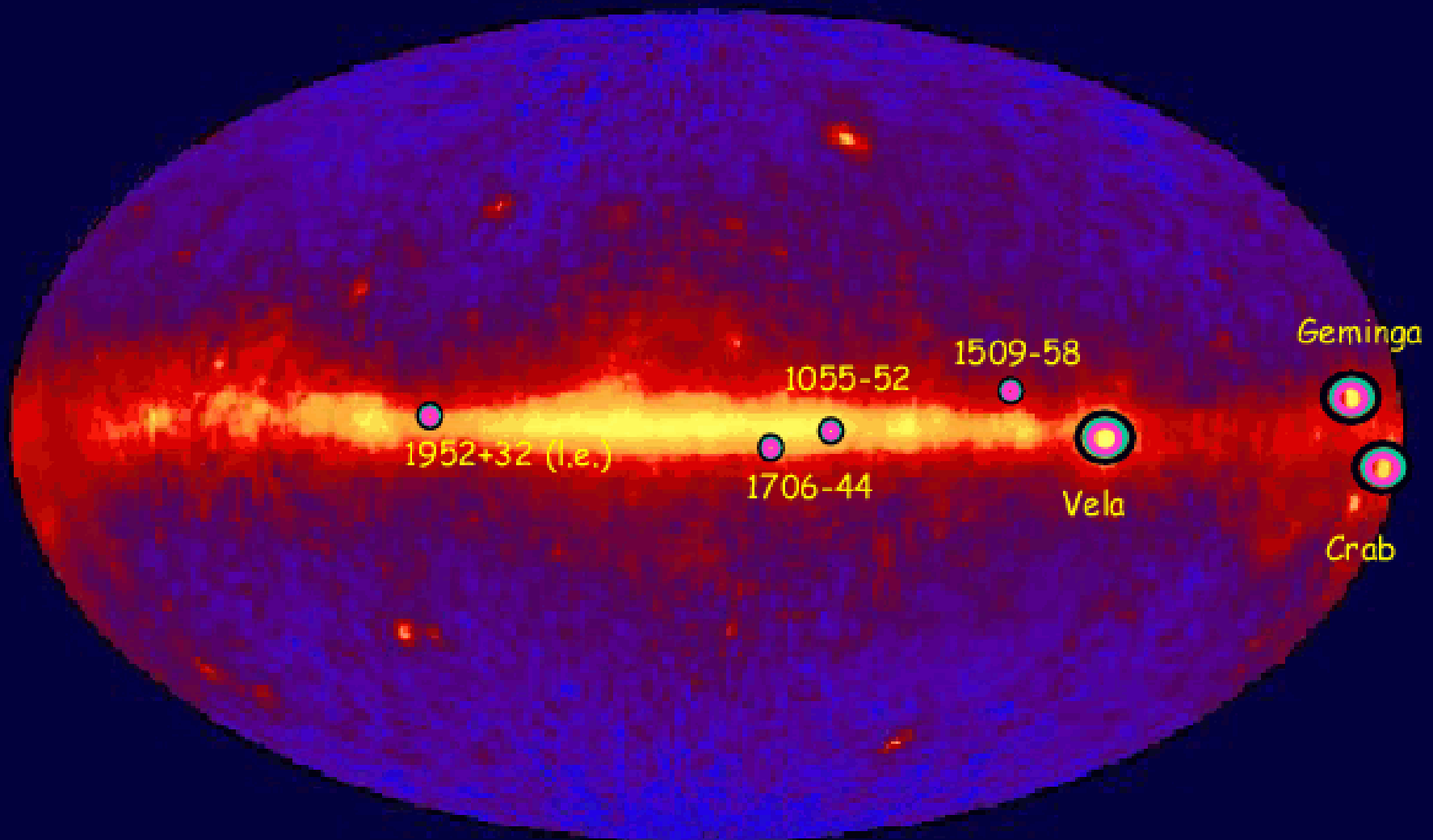
Gamma-ray pulsars

- **CGRO** (20 keV-30 GeV) heritage: number of γ -ray pulsars increased from 2 (Crab, Vela) to 7 (10)
- (10) include with lower significances also:
PSR B0144+59,
PSR B0656+14,
PSR J0218+4232 (ms-psr!)
- All relatively young (\leq few 100 kyr) and energetic
- Established Galactic γ -ray source population, emitting over a wide high-energy range (0.5 keV – 10 GeV)

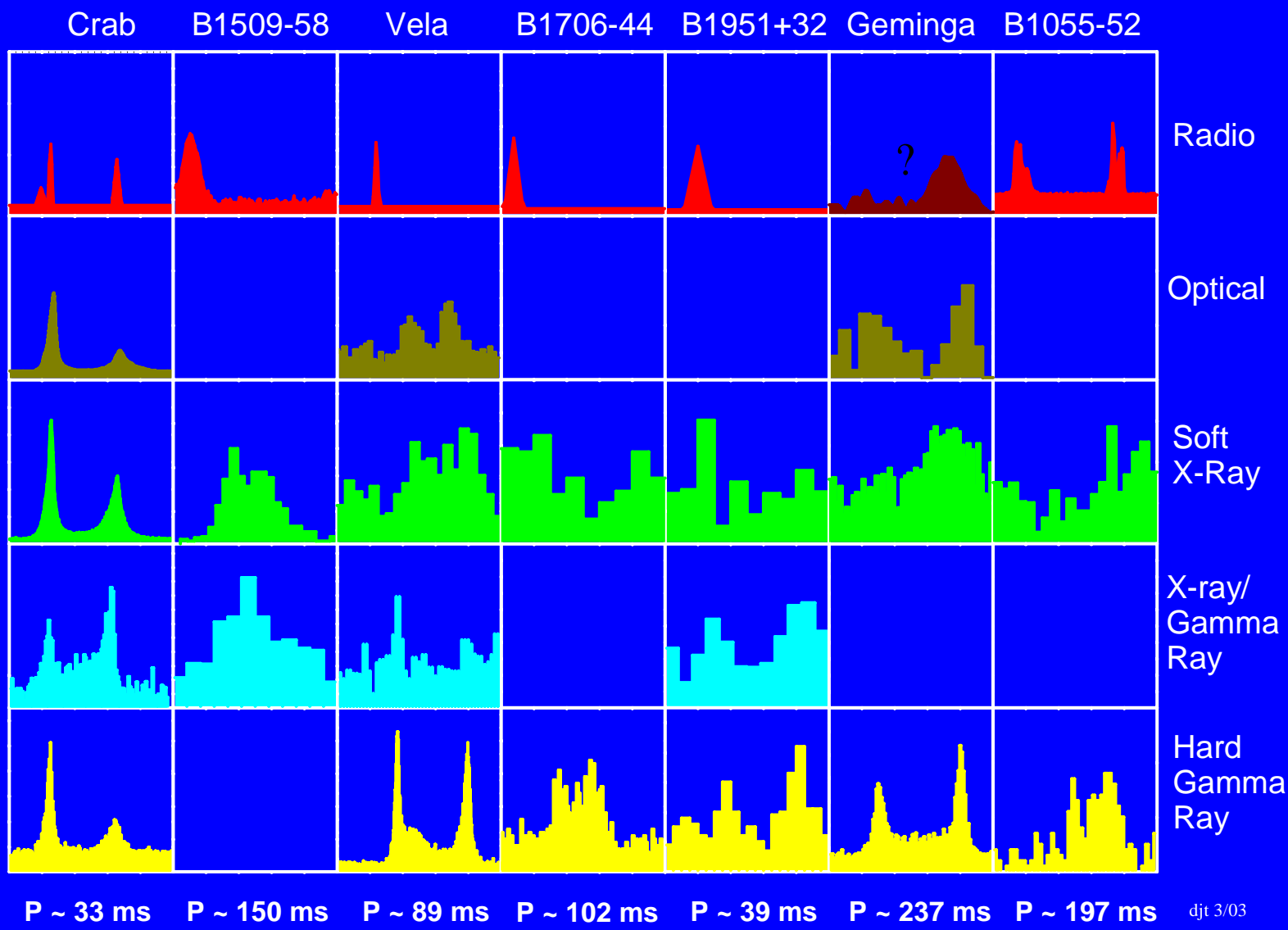


Thompson, Harding, Hermsen, Ulmer, 1997

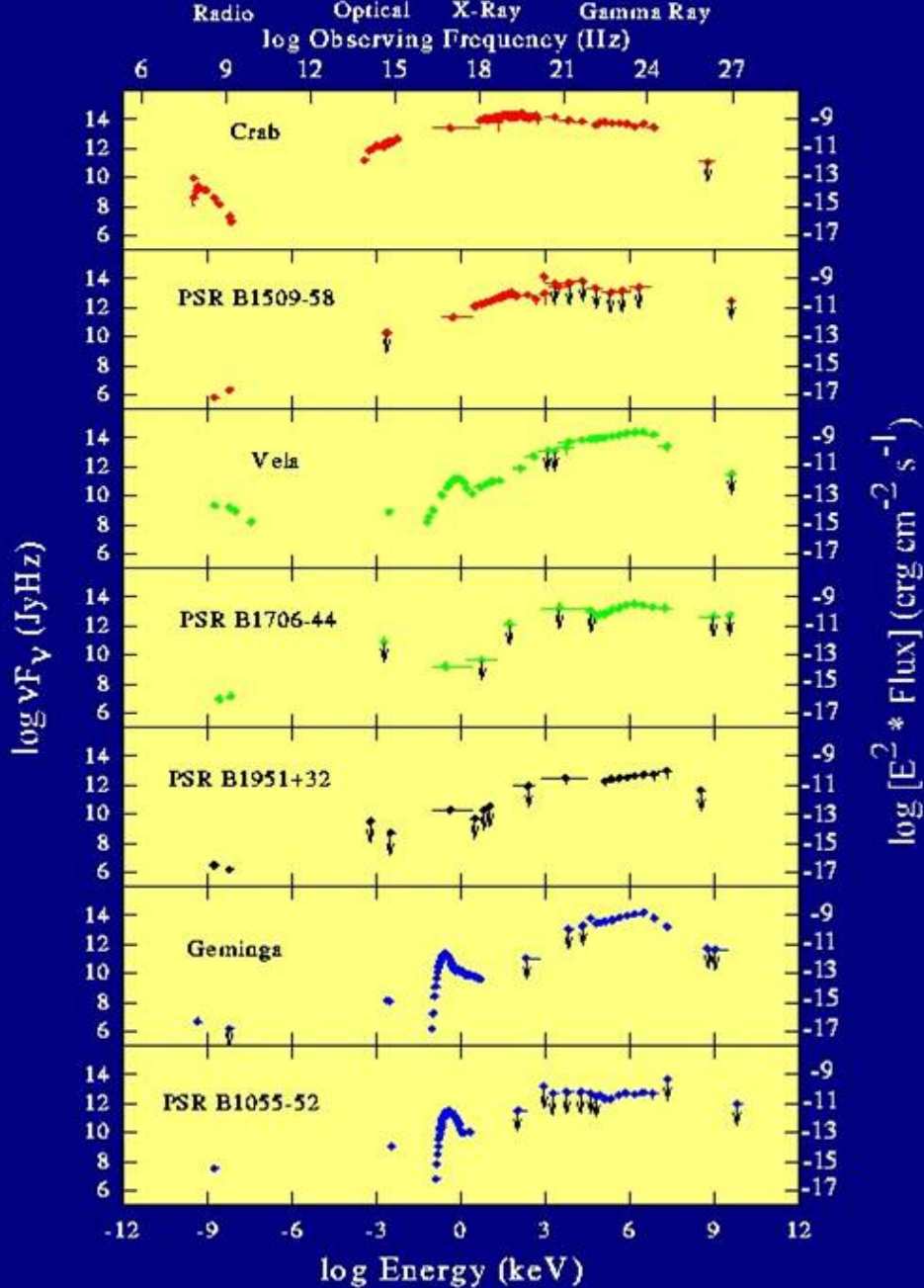
The seven highest-confidence gamma-ray pulsars on an EGRET all-sky map for $E > 100$ MeV



Intensity variation during one rotation of the neutron star



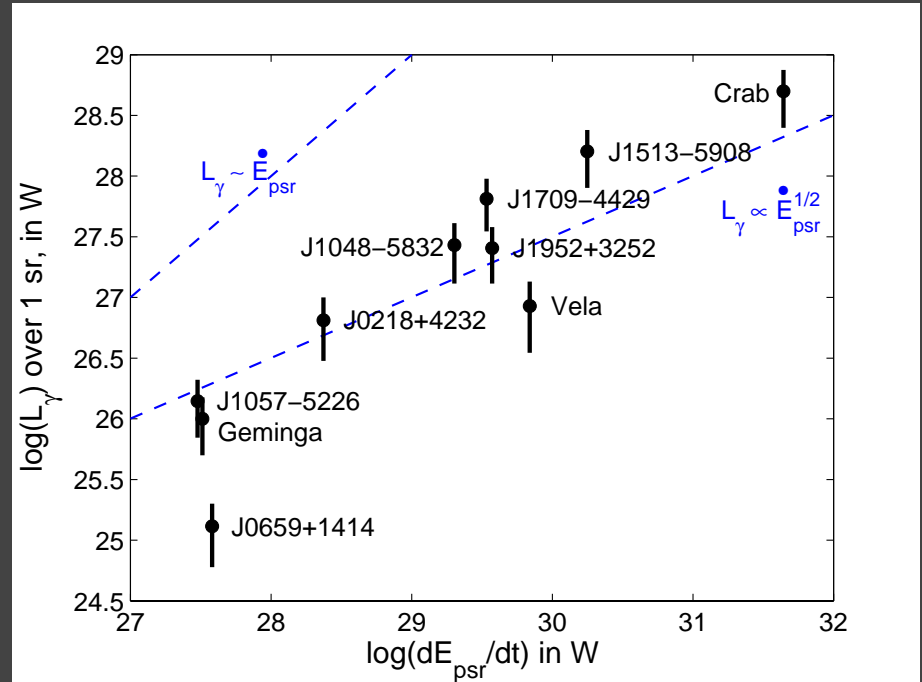
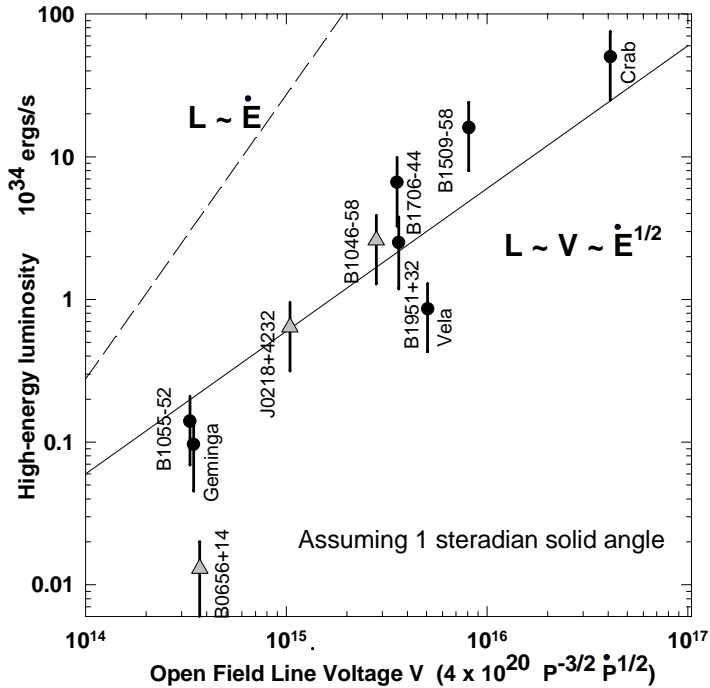
djt 3/03



Multiwavelengths spectra of pulsed emission

- Power peaks in γ -rays (hard X-rays for Crab)
- No pulsed emission above 20 GeV
- High-energy turnover
- Middle-aged pulsars show multiple thermal X-ray components:
cool BB $T \sim 0.5 - 1$ MK
hot BB $T > 1$ MK (old+msp)
- For young pulsars non-thermal X-rays dominate

Correlation studies: Are they meaningful using this small sample?



$$L_x \sim 10^{-3} \dot{E} \quad (\text{with large scatter})$$

For all model scenario's measured values depend strongly on combination of inclination angle α between magnetic and rotation axes, as well as the observers viewing angle ζ

Non-Thermal X-ray Detected Rotation-Powered Pulsars^a

| PSR | P (ms) | \dot{P} ($10^{-15} \text{ s s}^{-1}$) | d (kpc) | $\log(B)$ (G) | $\log(\tau_c)$ (yr) | $\log(\dot{E})$ (erg s^{-1}) | $\log(L_x)^p$ (erg s^{-1}) | $\log(L_x)^t$ (erg s^{-1}) | Detections | | | Telescope | Reference |
|------------|-----------|--|--------------|------------------|------------------------|--|--|--|------------|---|----------|-------------------|-------------------------|
| | | | | | | | | | R | O | γ | | |
| J1846-0258 | 324.00 | 7097.1 | 19 | 13.99 | 2.88 | 36.92 | 34.61 | 36.32 | | | | <i>ASCA/RXTE</i> | Gotthelf et al. 2000 |
| B0531+21 | 33.40 | 421 | 2 | 12.88 | 3.12 | 38.65 | 35.85 | 37.02 | X | X | X | <i>ASCA</i> | Saito 98 |
| B1509-58 | 150 | 1536 | 4.3 | 13.49 | 3.21 | 37.26 | 34.60 | 34.80 | X | X | X | <i>ASCA</i> | Saito 98 |
| B0540-69 | 50 | 479 | 49.4 | 13.00 | 3.24 | 38.18 | 36.10 | 36.92 | X | X | | <i>ASCA</i> | Saito 98 |
| J1930+1852 | 136 | 750.57 | 5.00 | 13.31 | 3.48 | 37.07 | 32.63 | | X | | | <i>Chandra</i> | Camilo et al. 02 |
| J0537-6910 | 16.10 | 51.2 | 49.4 | 12.26 | 3.72 | 38.69 | 35.52 | | | | | <i>RXTE</i> | Marshall et al. 98 |
| J0205+6449 | 65.70 | 193 | 2.6 | 12.86 | 3.75 | 37.43 | | 32.20 | X | | | <i>Chandra</i> | Murray et al. 02 |
| J1617-5055 | 69 | 140 | 3.3 | 12.80 | 3.91 | 37.23 | 33.48 | 33.76 | X | | | <i>ASCA</i> | Torii et al. 98 |
| J2229+6114 | 52 | 78.300 | 3 | 12.61 | 4.04 | 37.34 | | 33.01 | X | | | <i>ASCA</i> | Halpern et al. 01 |
| B0833-45 | 89 | 124 | 0.25 | 12.83 | 4.08 | 36.84 | 31.60 | 32.70 | X | X | X | <i>RXTE</i> | Harding et al. 02 |
| J1420-6048 | 68 | 83.167 | 7.69 | 12.68 | 4.13 | 37.02 | 34.46 | | X | | | <i>ASCA</i> | Roberts et al. 01 |
| B1800-21 | 134 | 134 | 3.94 | 12.93 | 4.22 | 36.34 | | 33.06 | X | | | <i>ROSAT</i> | Becker & Trümper 97 |
| B1706-44 | 102 | 92.2 | 1.43 | 12.79 | 4.27 | 36.54 | 32.16 | 33.15 | X | | X | <i>Chandra</i> | Gotthelf et al. 02 |
| J1811-1926 | 64.70 | 44 | 5 | 12.53 | 4.39 | 36.81 | 34.39 | | | | | <i>ASCA</i> | Torii et al. 97 |
| B1951+32 | 39.53 | 5.837 | 2.5 | 11.99 | 5.05 | 36.57 | | 33.79 | X | | X | <i>ASCA</i> | Saito 98 |
| B0656+14 | 384 | 55 | 0.76 | 12.97 | 5.07 | 34.59 | 30.26 | 32.98 | X | X | X | <i>ASCA</i> | Greiveldinger et al. 96 |
| Geminga | 237 | 11.4 | 0.16 | 12.52 | 5.54 | 34.53 | 29.56 | 29.79 | X | X | X | <i>ASCA</i> | Halpern & Wang 97 |
| B1055-52 | 197 | 5.8 | 1.38 | 12.34 | 5.75 | 34.48 | 29.48 | 33.42 | X | X | X | <i>ASCA</i> | Greiveldinger et al. 96 |
| B1929+10 | 226 | 1.15E+00 | 0.17 | 12.01 | 6.52 | 33.60 | 29.51 | 30.00 | X | X | | <i>ASCA</i> | Saito 98 |
| B1821-24 | 3 | 1.60E-03 | 5.5 | 9.65 | 7.49 | 36.37 | 31.80 | 33.24 | X | | | <i>ROSAT</i> | Becker & Trümper 97 |
| B1937+21 | 1.55 | 1.00E-04 | 3.60 | 8.90 | 8.41 | 36.03 | 31.66 | 32.8 | X | | | <i>BeppoSax</i> | Nicastro et al. 03 |
| J0218+4232 | 2.32 | 7.50E-05 | 5.85 | 8.93 | 8.71 | 35.38 | 32.11 | 32.75 | X | | X | <i>ROSAT</i> | Kuiper et al. 98 |
| J0437-4715 | 5.75 | 5.70E-05 | 0.18 | 9.06 | 9.23 | 34.08 | 30.48 | 30.86 | X | | | <i>Chandra</i> | Zavlin et al. 02 |
| J2124-3358 | 4.93 | 1.10E-05 | 0.25 | 8.67 | 9.87 | 33.56 | 29.80 | 30.35 | X | | | <i>ROSAT/ASCA</i> | Becker & Trümper 99 |
| J0030+0451 | 4.86 | 1.00E-05 | 0.23 | 8.65 | 9.91 | 33.54 | 30.26 | | X | | | <i>ROSAT</i> | Becker & Trümper 99 |

^a $(L_x)^p$ is pulsed, non-thermal X-ray flux and $(L_x)^t$ is total X-ray flux.

Recent compilation by Kaspi

Thermally Cooling Young Rotation-Powered Pulsars^a

| Pulsar Name | SNR | τ_c /SNR Age (kyr) | d (kpc) | N_h (10^{21} cm^{-2}) | kT^∞ (eV) | R^∞ (km) | L^∞ ^c (erg s^{-1}) | Model ^b | Telescope | Reference ^d |
|-----------------------|-------------|-------------------------|-----------|-------------------------------------|------------------|-----------------|---|--------------------|-----------------------|------------------------|
| J0205+6449 | 3C 58 | 5.4/0.82 | (3.2) | (3.86) | <93 | (12) | $< 1.4 \times 10^{33}$ | BB | <i>Chandra</i> | Slane et al. 2002 |
| B0355+54 | - | 562/- | (2.1) | (2) | 82 ± 4 | (10) | $5.8 \pm 0.3 \times 10^{32}$ | BB | <i>ROSAT/Einstein</i> | Slane 94 |
| B0531+21 | Crab | 1.3/0.949 | (2) | (3) | < 172 | (15.6) | $< 2.7 \times 10^{34}$ | BB | <i>Chandra</i> | Weisskopf et al 03 |
| J0538+2817 | S147 | 620/~100 | (1.2) | 4.7 ± 0.2 | 54 ± 1 | 13 | 2×10^{32} | <i>B-H</i> | <i>Chandra</i> | Romani & Ng 03 |
| J0633+1746 | - | 340/- | 0.16 | 0.08–0.18 | 38–54 | 4–8 | $1.5\text{--}1.7 \times 10^{31}$ | BB | <i>ASCA/ROSAT</i> | Halpern & Wang 97 |
| B0656+14 ^e | - | 110/- | 0.288 | 0.17 ± 0.02 | 69 ± 3 | 8.5 | 2.1×10^{32} | BB | <i>Chandra</i> | Brisken et al. 03 |
| B0833–45 | Vela | 11/~10 | 0.21 | 0.33 ± 0.03 | 57 ± 3 | (13) | $2.6 \pm 0.2 \times 10^{32}$ | <i>B-H</i> | <i>Chandra</i> | Pavlov et al. 01 |
| B1055–52 ^e | - | 540/- | (0.7) | ? | 65 | 13 | 3.8×10^{32} | BB | <i>Chandra</i> | Pavlov & Zavlin 03 |
| B1706–44 | G343.1–2.3? | 17.4/? | (1.8) | (2.5) | < 94 | (10.4) | $< 1.8 \times 10^{33}$ | BB | <i>ROSAT</i> | Becker et al. 95 |
| J1811–1925 | G11.2–0.3 | 24/2 | (5) | (21.3) | < 150 | (10) | 6.5×10^{33} | BB | <i>Chandra</i> | Roberts 03 |
| B1823–13 | - | 21/- | (4) | (20) | < 147 | (12) | $< 8.7 \times 10^{33}$ | BB | <i>XMM</i> | Gaensler et al. 03 |
| B2334+61 | G114.3+0.3 | 41/? | (2.5) | (2) | < 72 | (10.4) | $< 6 \times 10^{32}$ | BB | <i>ROSAT</i> | Becker et al. 96 |

^aNumbers in parentheses represent values assumed by the authors.

^bBB is a blackbody model; *B-H* is a magnetic hydrogen atmosphere model.

^cAll luminosities are bolometric.

^dMost recent relevant reference; references contained therein may also be relevant.

^eThe spectrum is best fit with two blackbodies. We report here the softer of the two, as that component has inferred radius comparable to the size of the neutron star, as expected for whole-surface thermal emission.

Recent compilation by Kaspi

Most X-ray pulsars detected in “classical” X-ray range below 10 keV.

Observational gap between 10 keV and 100 MeV

Deep searches in archives and possibilities for currently operational missions.

Detection of only four normal pulsars published:

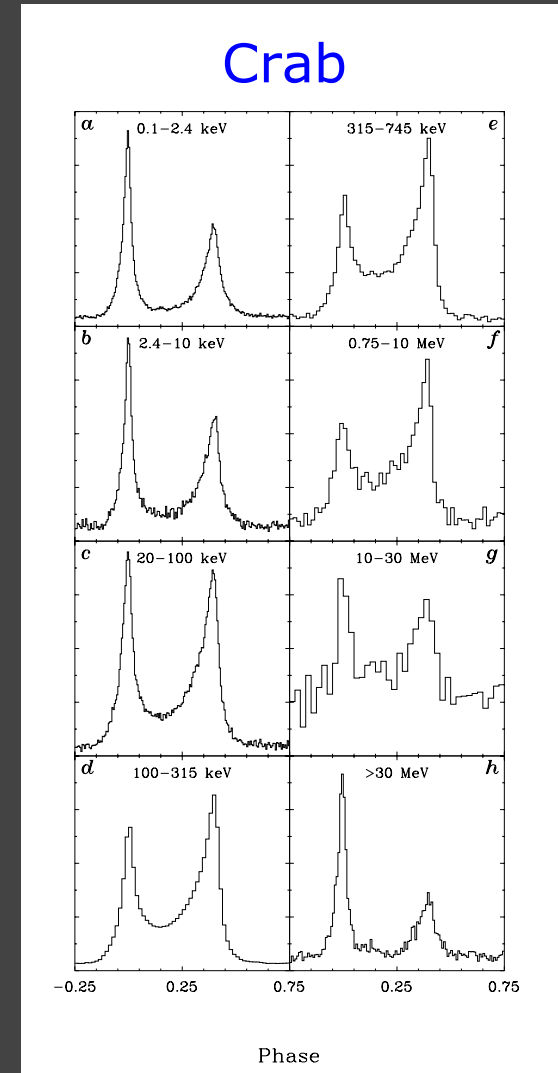
Crab

PSR B1509-58 (not above 100 MeV)

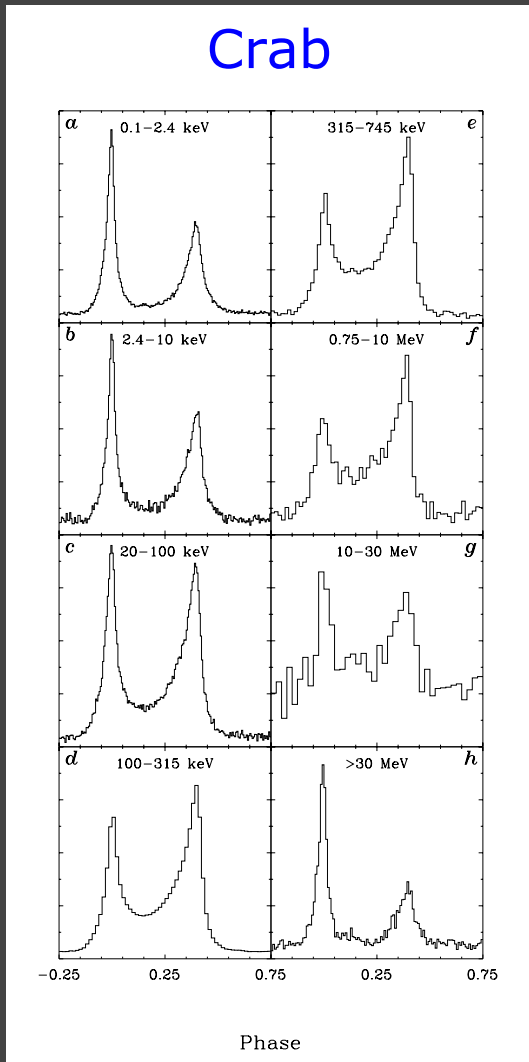
Vela

PSR B0540-69 (not above 50 keV)

Models are still mostly verified on Crab and Vela results, but not using all details!



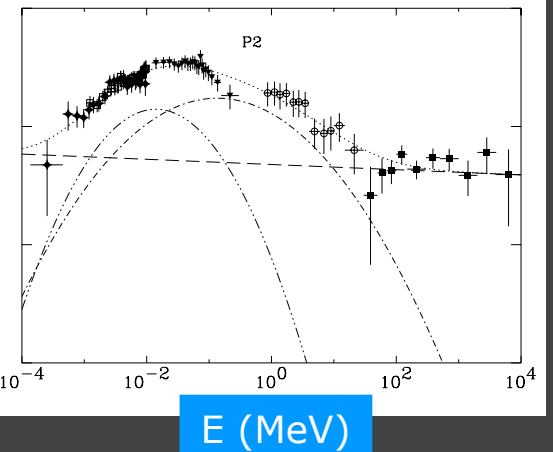
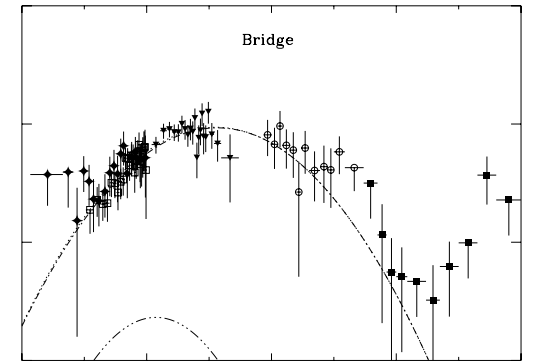
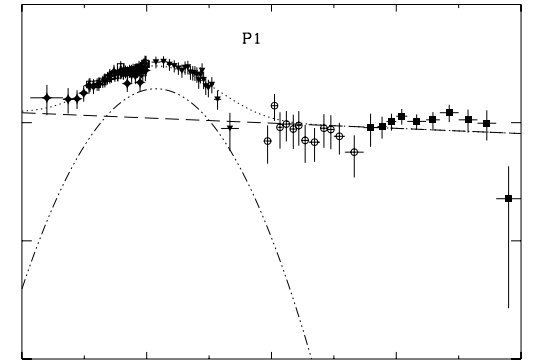
Crab: Phase-Resolved Spectroscopy



1st Peak P1

Bridge Emission

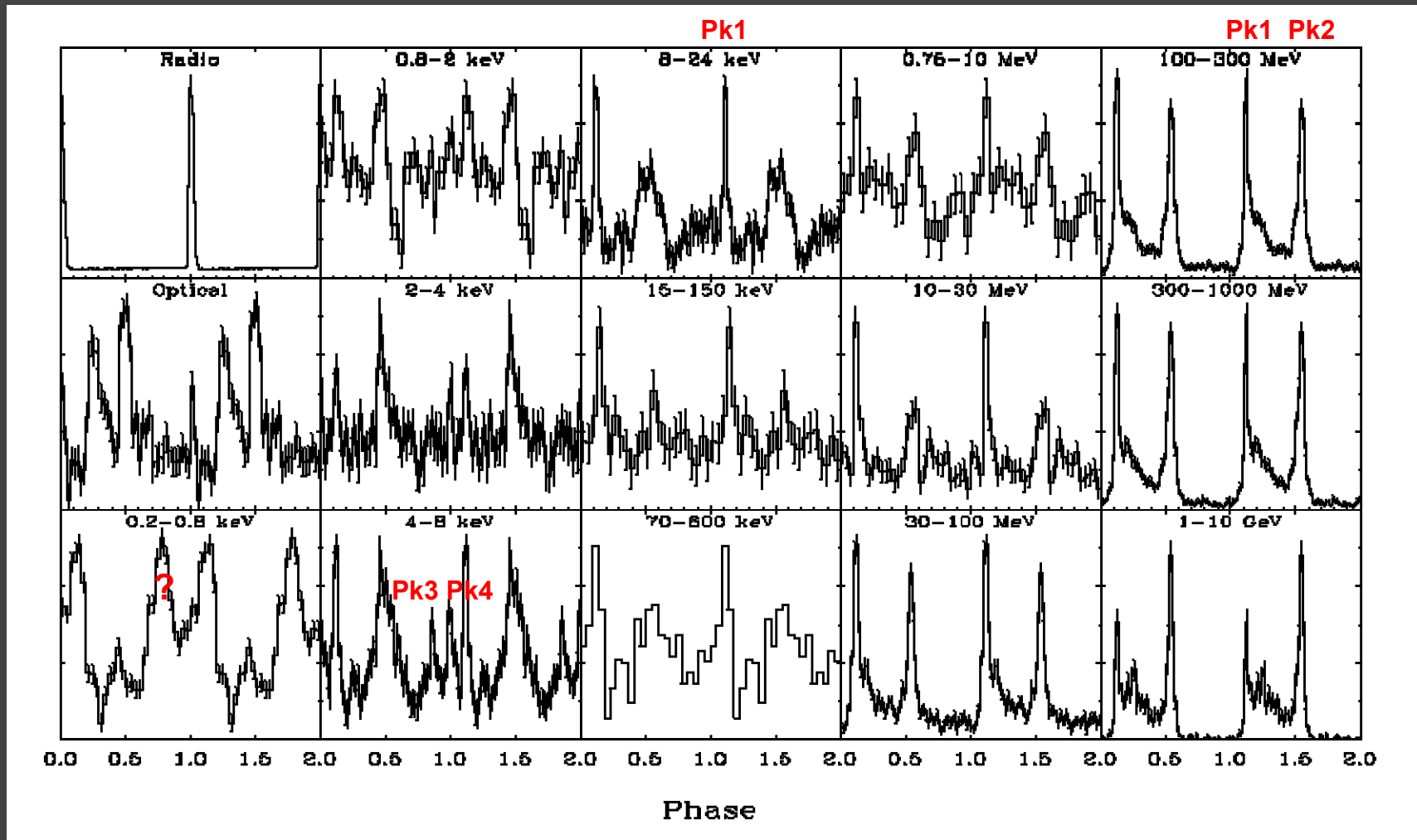
2nd Peak P2



Vela pulse profiles from radio up to high-energy gamma rays

Phase-resolved spectroscopy?

Hermesen & Kuiper 2006, in prep. A&A



Vela Pulsar in the Ultraviolet

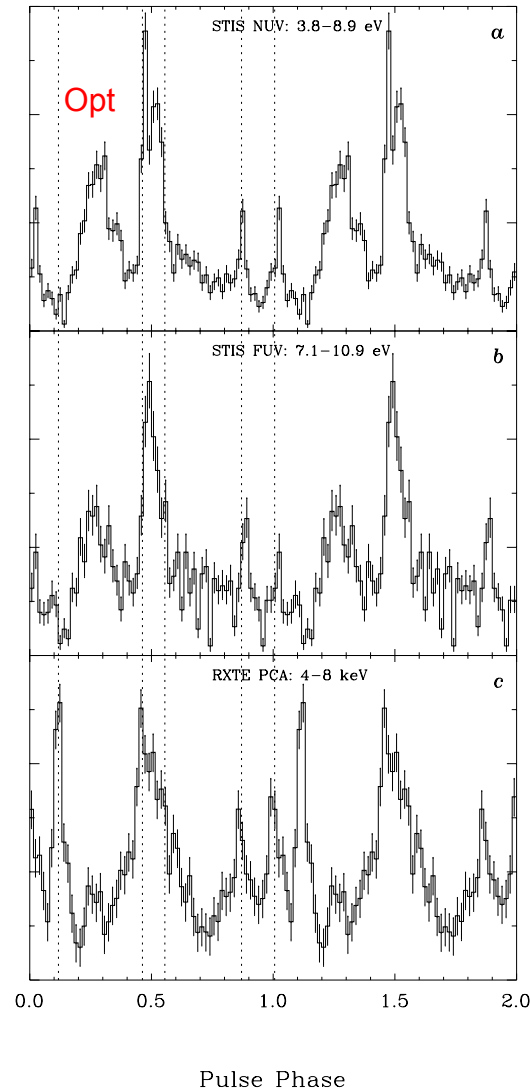
(Romani, Kargaltsev, Pavlov 2005)

- ▶ UV profiles also show sharp pulses (~ 1 ms) for Pk2/soft, Pk3, Pk4
- ▶ UV pulse at phase 1st Optical pulse
- ▶ New soft X-ray pulse (200-800 eV) at phase 0.78 NOT in UV (< 11 eV)
- ▶ Pk4 (\sim radio phase) Compton up-scatter of radio photons from center of polar cap?

OR

Pk4 \sim at phase of giant micro pulses, similar to PSR J1937+21, PSR B1821-24 and Crab: giant radio pulses at phases of non-thermal X-ray pulses

Pk 1 Pk2 Pk3 Pk4



3.8-8.9 eV

(UV absolute phase uncertain)

7.1-10.9 eV

4-8 keV

- Vela: Extremely structured high-energy phase histogram challenging the competing models
- Are all light curves this structured in the X-ray range?
- No, but we badly need more examples! Particularly to bridge the high-energy gamma-ray (> 100 MeV) results to the classical X-ray range below 10 keV
- Middle-aged pulsars are very weak hard X-ray emitters.

Rotation-Powered Young Pulsars

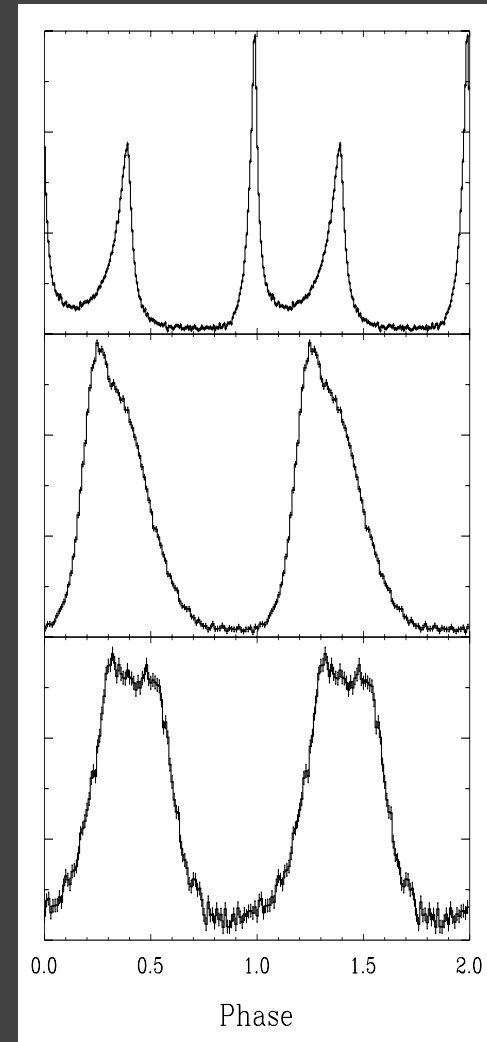
- Three young pulsars (< 10 kyr) at hard X-rays/soft γ -rays (*CGRO/RXTE/BeppoSAX*):

PSR B0531+21 (Crab)

PSR B1509-58

PSR B0540-69 ("twin"
of Crab in LMC)

- Different lightcurve shapes



Rotation-Powered Young Pulsars

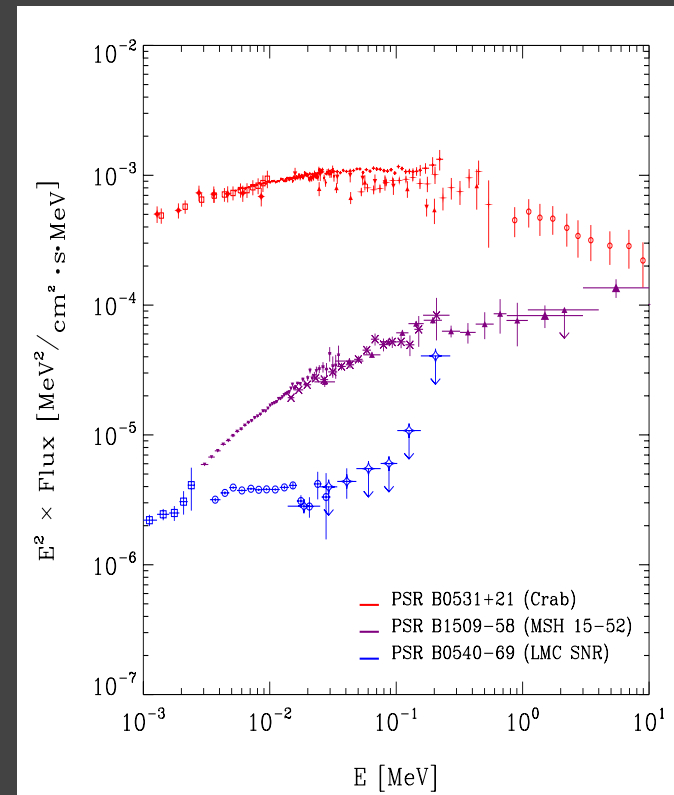
- Three young pulsars (< 10 kyr) at hard X-rays/soft γ -rays (*CGRO/RXTE/BeppoSAX*):

PSR B0531+21 (Crab)

PSR B1509-58

PSR B0540-69 (“twin” of Crab in LMC)

- HE-spectra are different from older γ -ray pulsars — L_x/L_γ larger !



Increased Sample of Young Rotation-Powered Pulsars emitting at hard X-ray energies (Kuiper & Hermsen in prep.2006)

- We selected radio-dim/quiet young rotation-powered pulsars located in/near SNR's:

PSR J1846-0258 (Kes 75)

PSR J1930+1852 (G54.1+0.3)

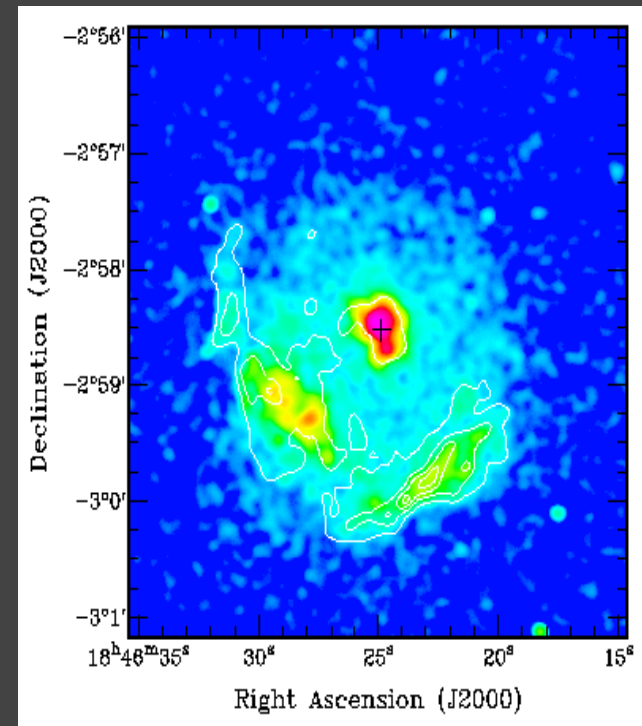
PSR J1811-1925 (G11.2-0.3)

PSR J1617-5055 (near RCW 103)

- Use of archival RXTE, BeppoSAX and ASCA data
- Follow-up with study with INTEGRAL

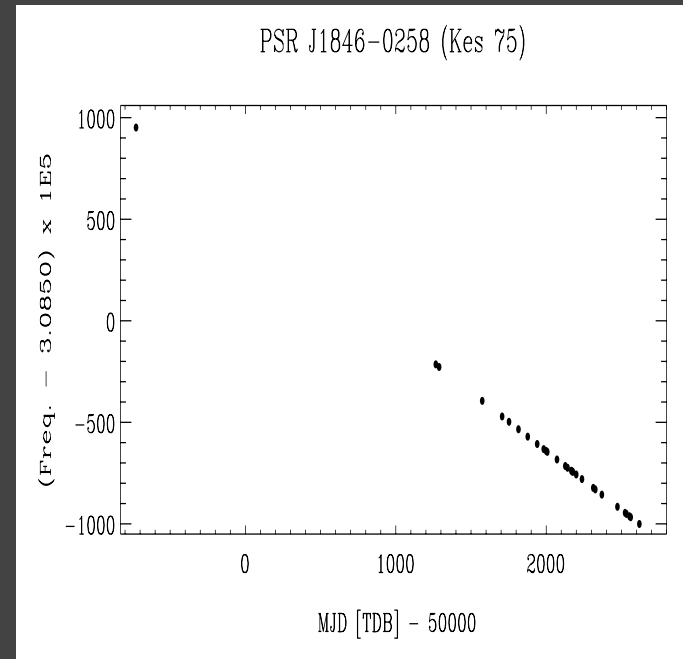
PSR J1846-0258 in SNR KES 75

- Discovered by Gotthelf et al. (2000) in RXTE and ASCA data
- “Slow” 324 ms pulsar; Characteristic age : 723 year
- Radio quiet rotation powered pulsar
- In centre of SN-remnant Kes-75 (G29.7-0.3)
(Chandra ACIS; Helfand et. al. 2003)



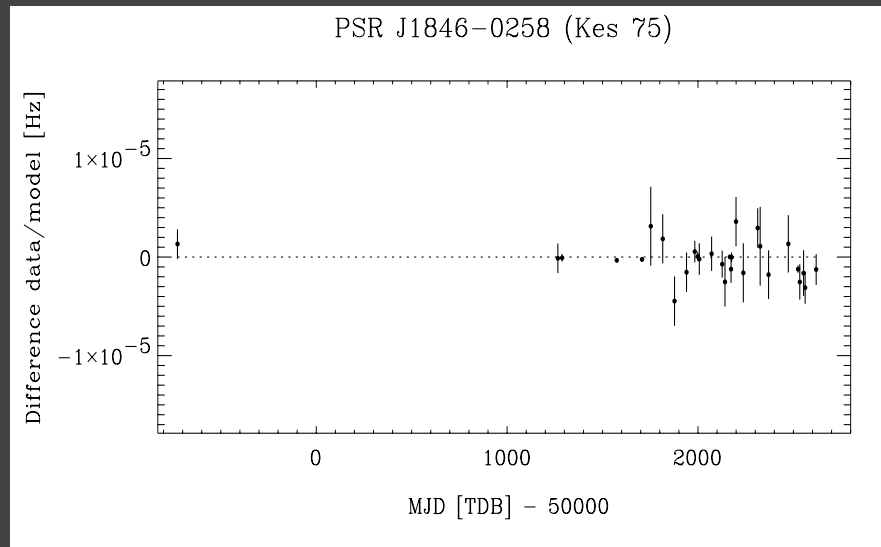
X-ray timing of the Kes-75 pulsar

- PSR J1846-0258 monitored regularly by RXTE PCA since its discovery
- Archival ASCA and BeppoSAX data
- Baseline ~ 9.2 y :
10-10-1993 – 25-01-2003
- Pulse period optimization per sub-observation using Z^2 -statistics



PSR J1846-0258 timing model

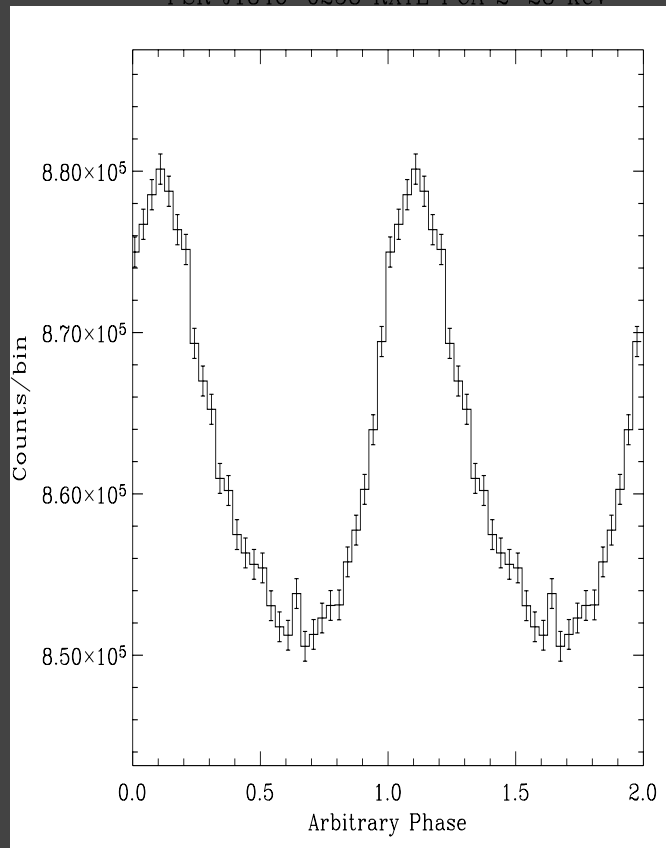
- Quadratic fit with ν_0 , $d\nu_0/dt$ and $d^2\nu_0/dt^2$ yields accurate fit parameters (χ^2_r of 1.28; d.o.f. 27)
- ν_0 : $3.07845283(5) \text{ s}^{-1}$
 $d\nu_0/dt$: $-6.7177(3) \times 10^{-15} \text{ s}^{-2}$
 $d^2\nu_0/dt^2$: $1.77(3) \times 10^{-21} \text{ s}^{-3}$
 t_0 : 52023 MJD TDB



PSR J1846-0258 (Kes-75) using all available RXTE PCA/HEXTE data

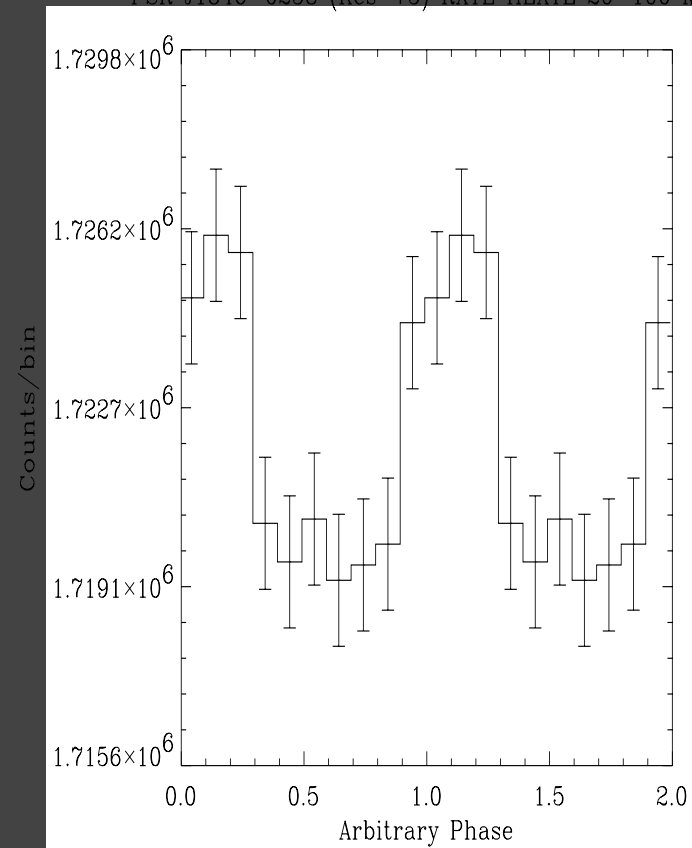
RXTE PCA (2-20 keV) $\sim 35\sigma$

PSR J1846-0258 RXTE PCA 2-28 keV



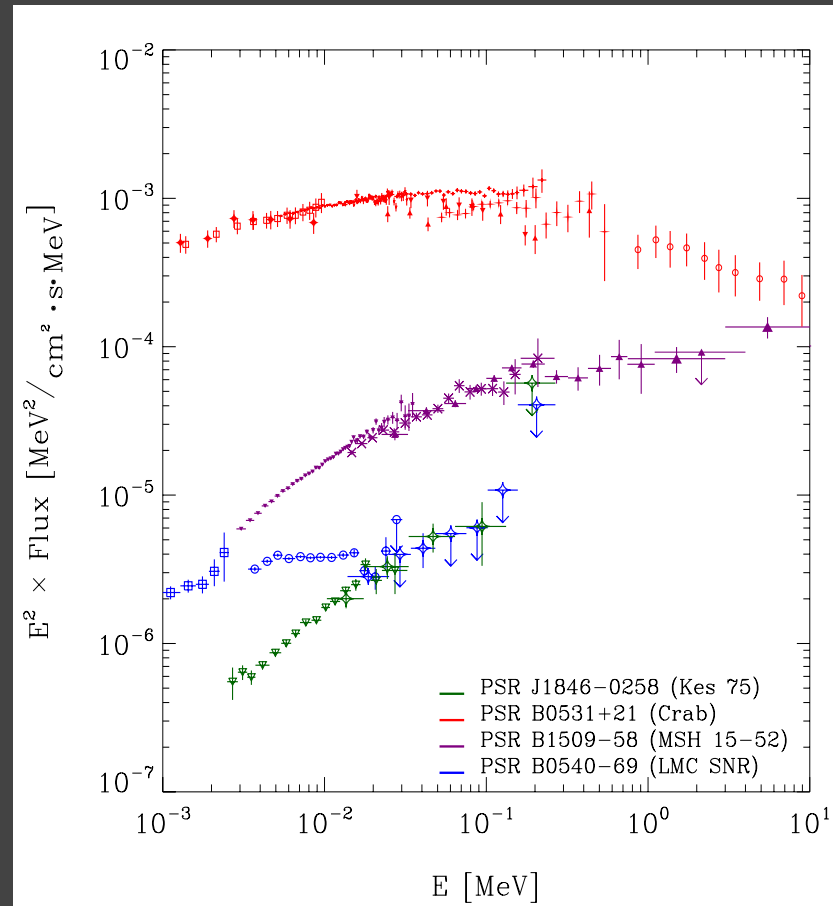
RXTE HEXTE (20-100 KeV) $\sim 6\sigma$

PSR J1846-0258 (Kes-75) RXTE HEXTE 20-100 keV



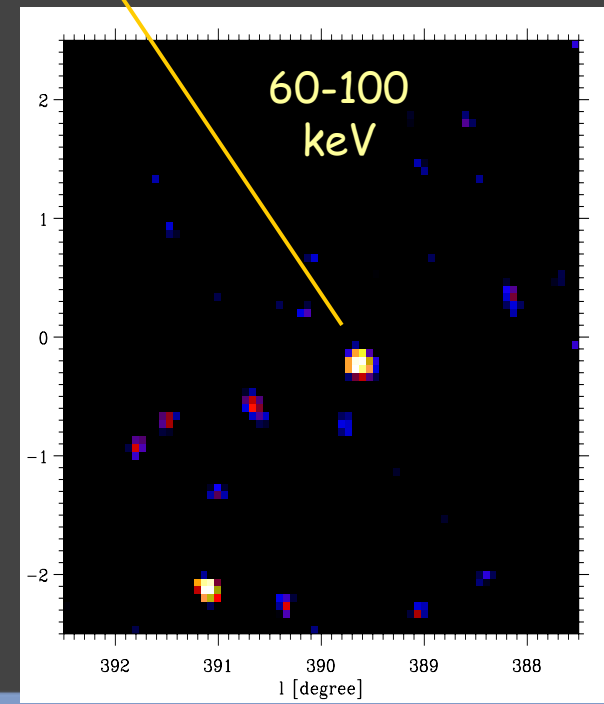
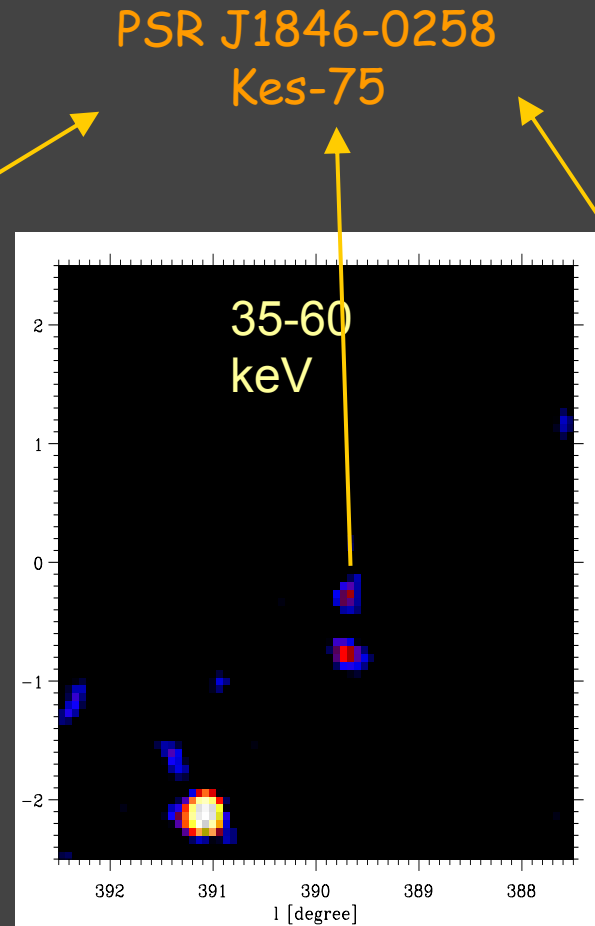
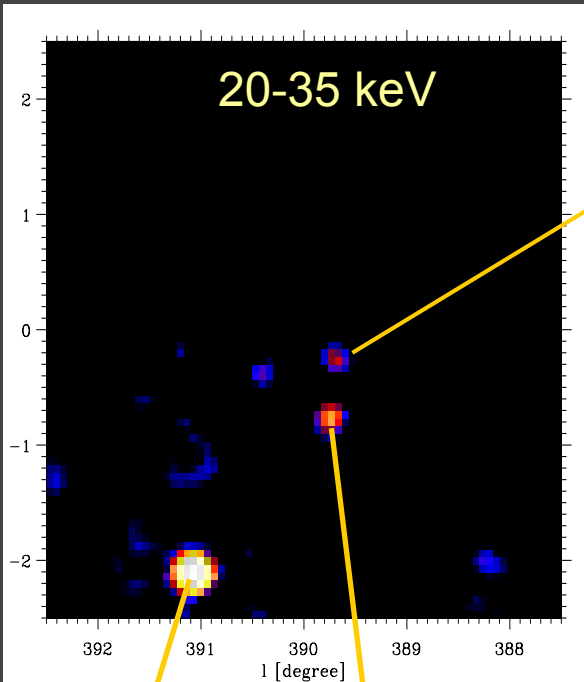
PSR J1846-0258 X-ray/soft gamma-ray spectrum RXTE PCA/HEXTE (407 ks PCA exposure)

- 2-30 keV: Photon index $\gamma \sim 1.07(1)$!
 $N_{\text{H}} = 3.96 \cdot 10^{22} \text{ cm}^{-2}$ (Helfand et al. 2003)



INTEGRAL IBIS ISGRI - GPS/GCDE

Kes-75: 480 ks within 10° of pointing



PSR J1846-0258
Kes-75

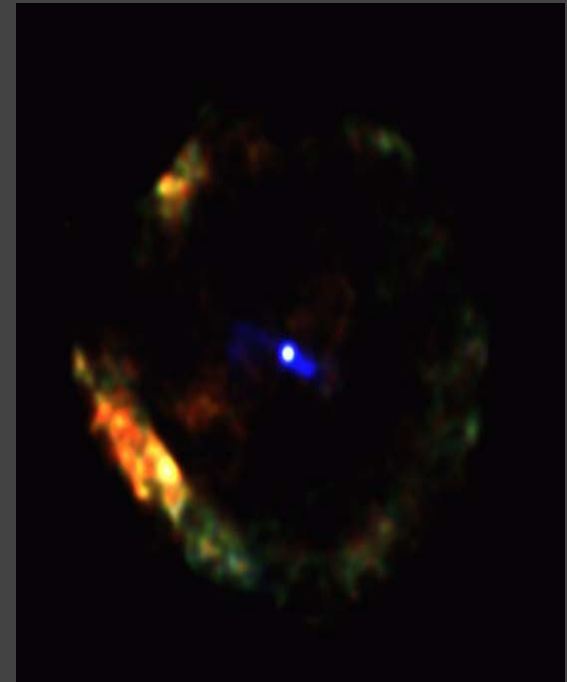
XTE J1855-026

IGR J18483-0311

Hard X-ray/soft γ -ray emission is composed of contributions from the PWN and pulsar

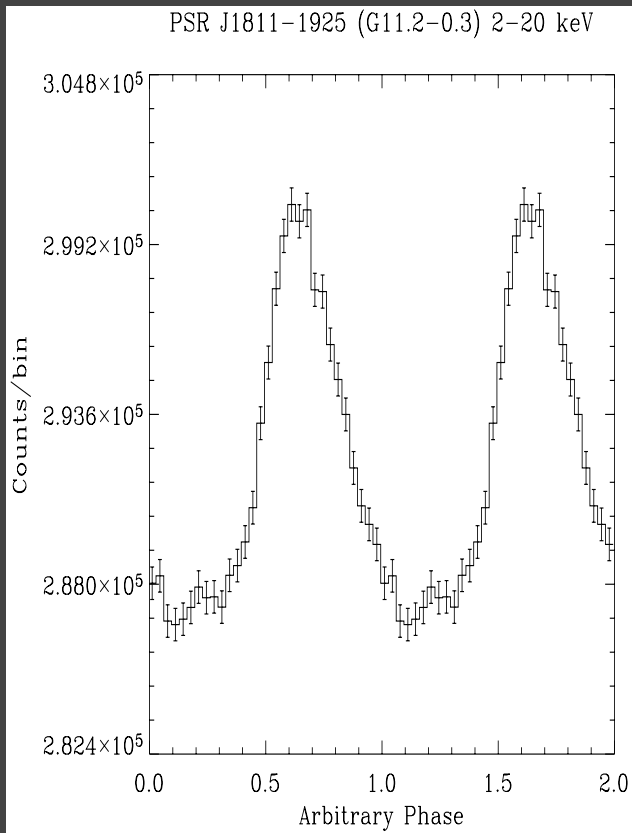
PSR J1811-1925 (G11.2-0.3)

- Discovered by Torii et al. (1997) in ASCA data (April 1994)
 - Fast 65 ms pulsar; Char. age : 24 kyr
 - Radio quiet rotation powered pulsar
 - In centre of SN-remnant G11.2-0.3 (Chandra ACIS Kaspi et al. 2001)
- Age remnant ~ 2 kyr

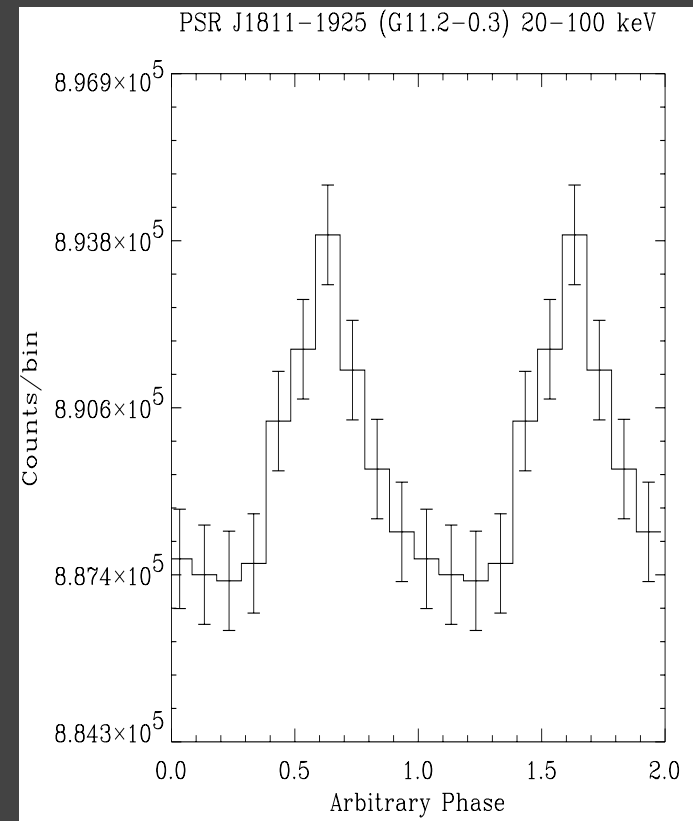


PSR J1811-1925 (G11.2-0.3) using 175 ks archival RXTE PCA/HEXTE data

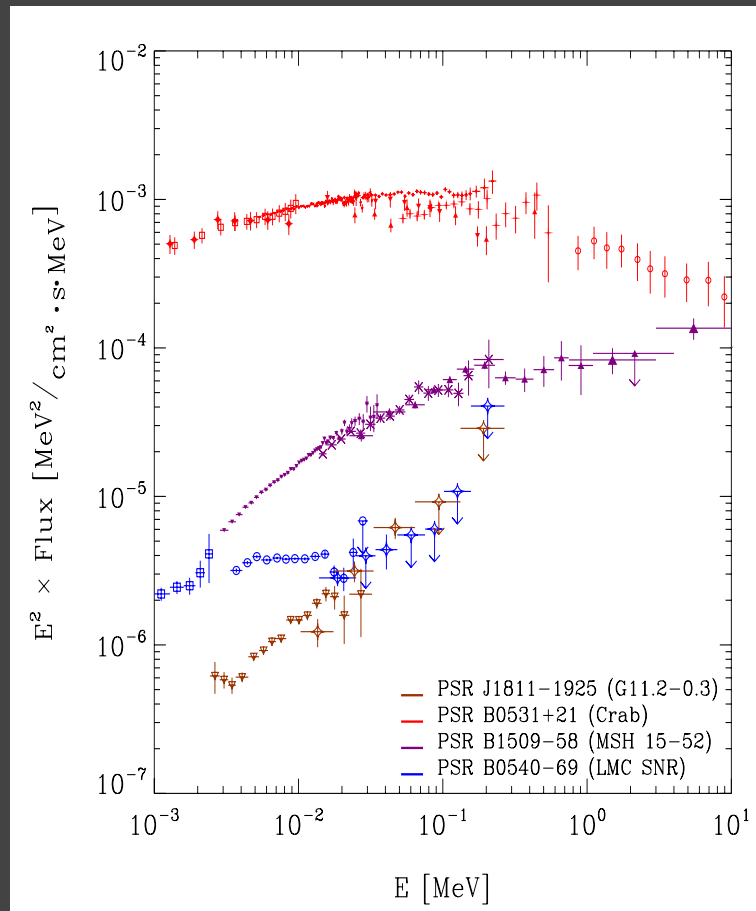
RXTE PCA 35 σ



RXTE HEXTE 6.3 σ



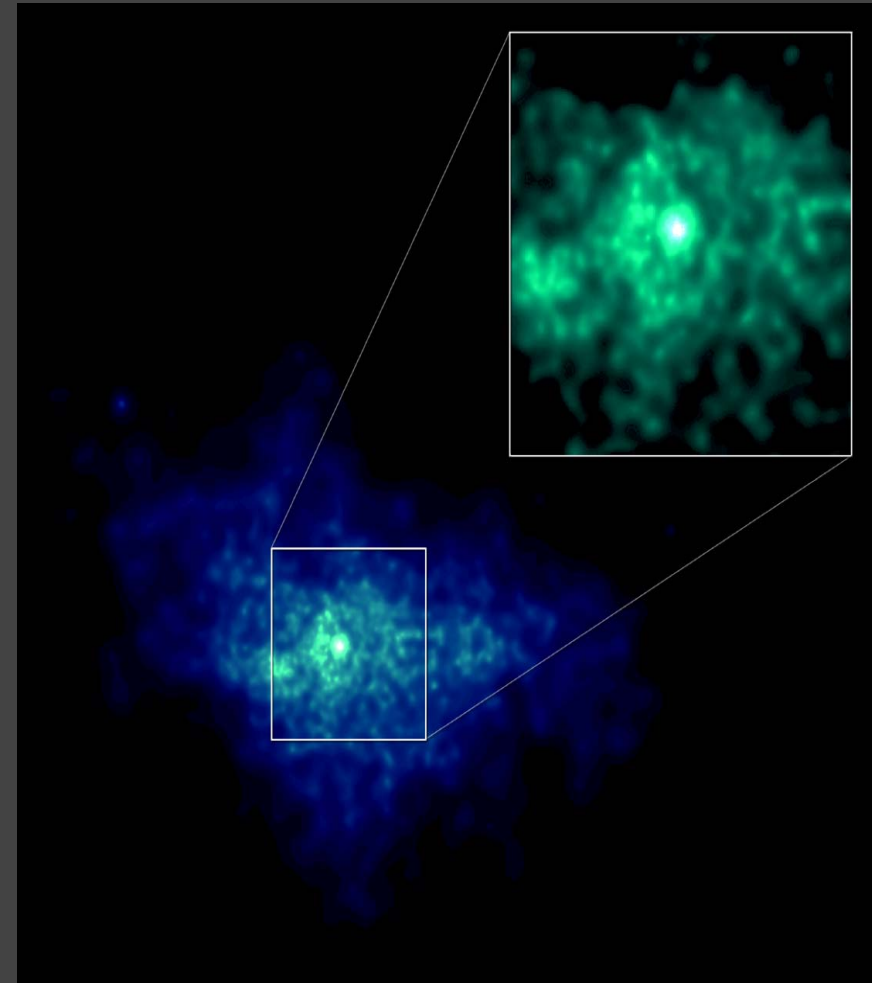
PSR J1811-1925 (G11.2-0.3) using 175 ks archival RXTE PCA/HEXTE data



- Spectral analysis 2-30 keV: Photon-index ~ 1.17 (1)
 $N_{\text{H}} = 2.36 \cdot 10^{22} \text{ cm}^{-2}$ (fixed; Roberts et al. 2003)

PSRJ1930+1852 (G54.1+0.3)

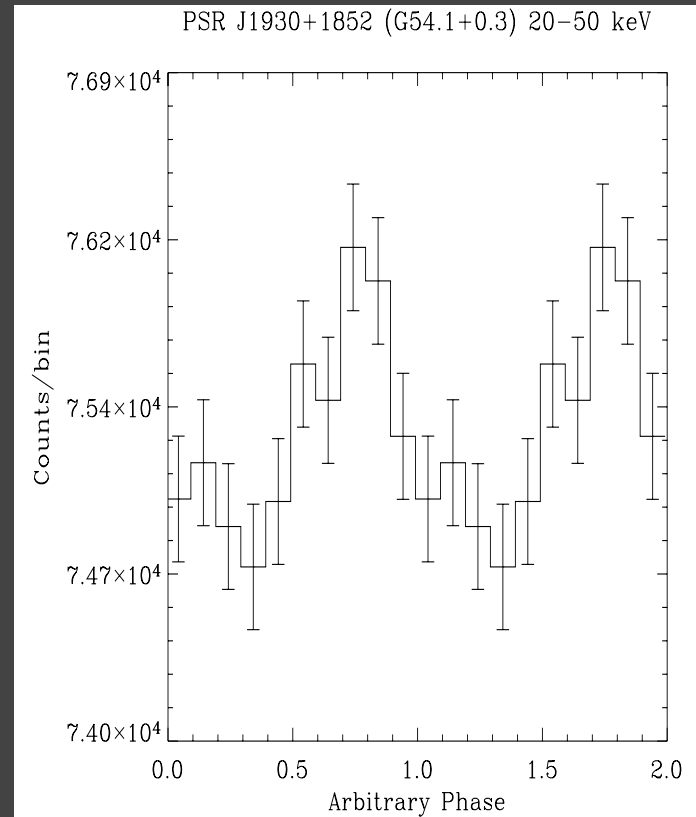
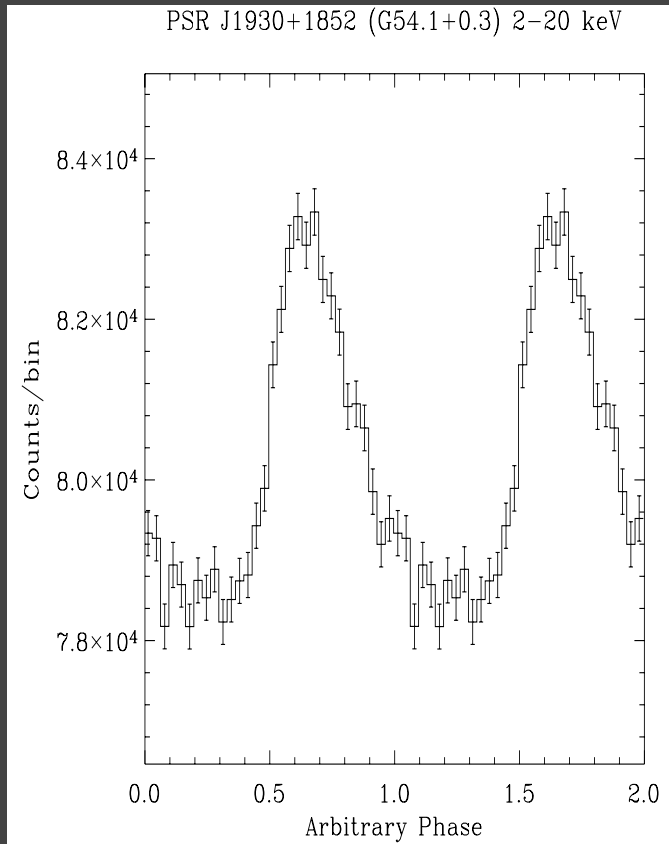
- Discovered by Camilo et al. (2002) at radio frequencies targetting at the central X-ray point-source in G54.1+0.3 (Chandra ACIS; Lu et al. 2002)
- Radio dim: $\sim 60\text{mJy}$; $P=136\text{ ms}$; char. Age $\sim 2,900\text{ y}$
- X-ray pulsations in archival (April 1997) ASCA GIS data; Single pulse profile
- Four frequency measurements as a function of time (ASCA, radio, RXTE PCA (2x)) over 5.6 yr rendered accurate ephemeris



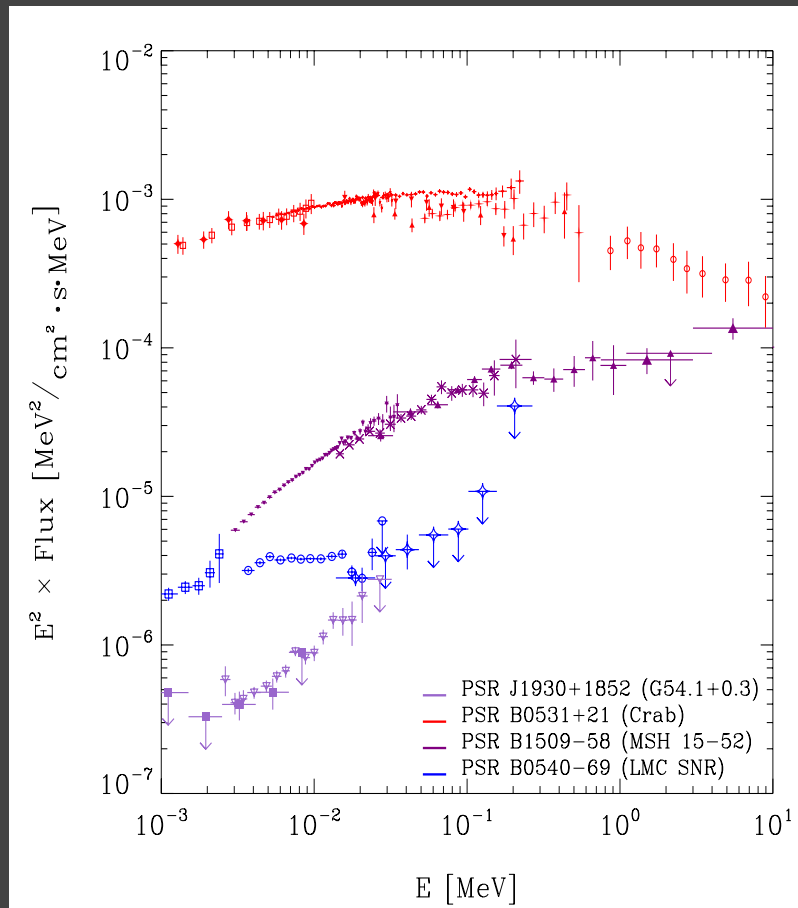
PSR J1930+1852 (G54.1+0.3) using recent RXTE PCA/HEXTE data (~ 80 ks)

RXTE PCA 31.9σ

RXTE HEXTE 4.0σ



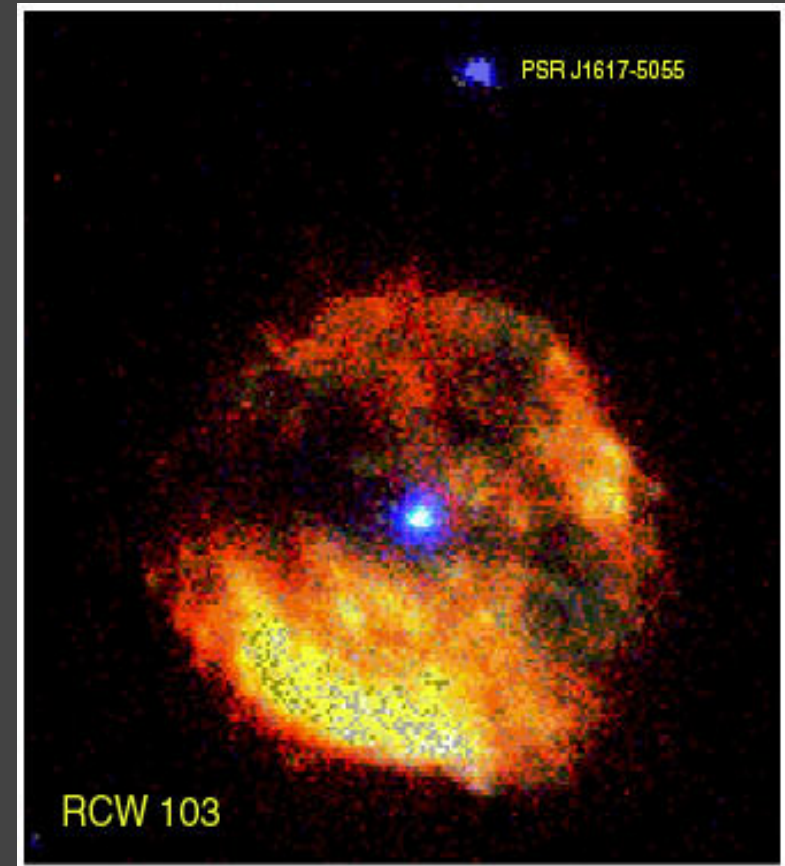
PSR J1930+1852 (G54.1+0.3) using recent RXTE PCA/HEXTE data (~ 80 ks)



- Spectral analysis 2-30 keV: Photon index $\sim 1.21(2)$
 $N_{\text{H}} = 1.60 \cdot 10^{22} \text{ cm}^{-2}$ (fixed; Lu et al. 2002)

PSRJ1617-5055 (in RCW 103)

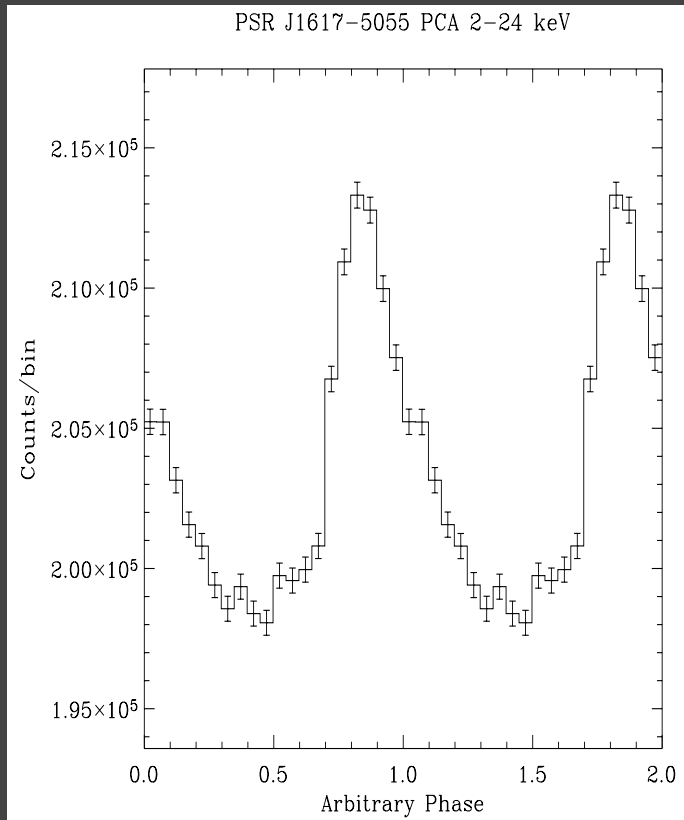
- Discovered at X-rays by Torii et al. (1998) in ASCA GIS data targeting on SNR RCW 103
- Radio dim: ~ 0.5 mJy; $P=69$ ms; char. Age $\sim 8,000$ y (Kaspi et al. 1998)



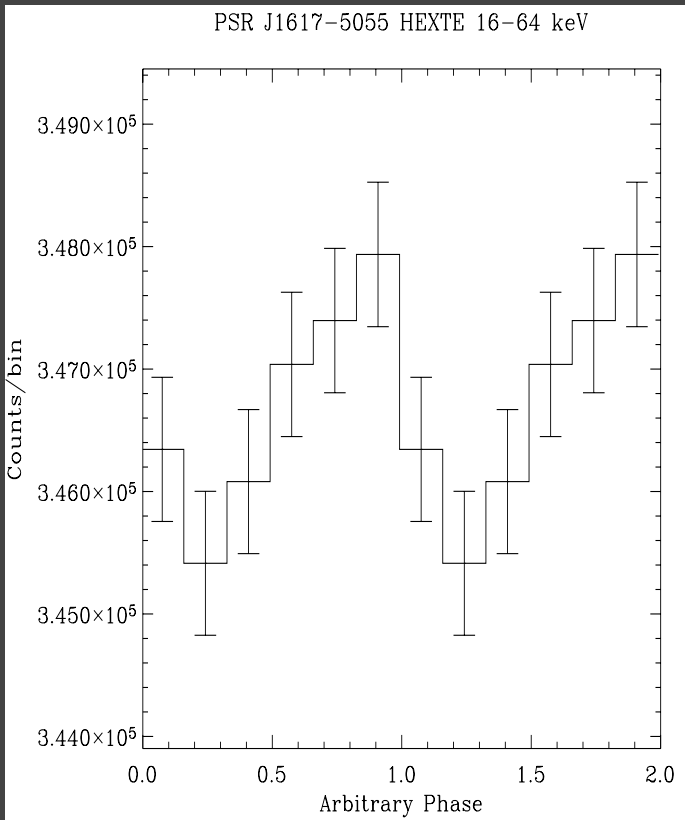
PSR J1617-5055

using RXTE PCA (P30210; ~67 ks) / HEXTE (~22 ks) data

RXTE PCA 34.5σ

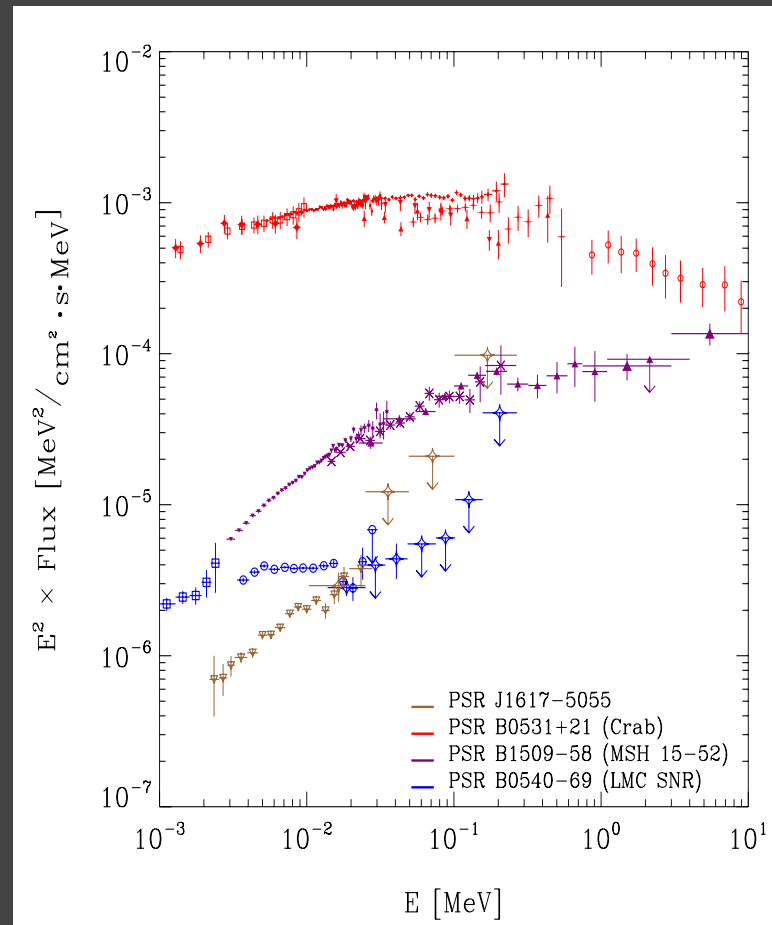


RXTE HEXTE 3.1σ



PSR J1617-5055

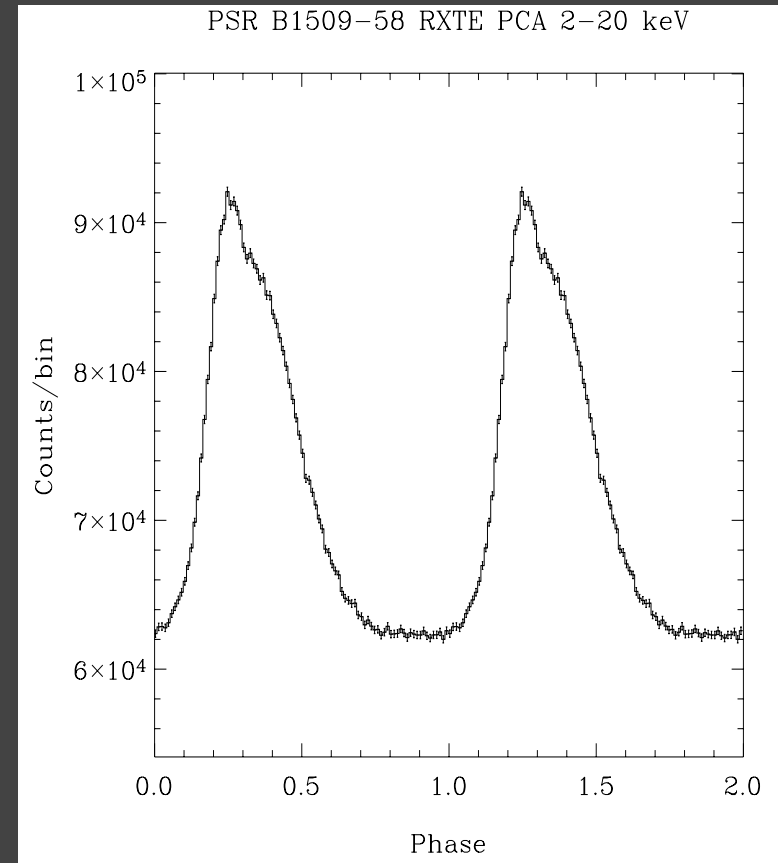
using RXTE PCA (P30210; ~67 ks) / HEXTE (~22 ks) data



- Spectral analysis 2-30 keV: Photon index $\sim 1.30(1)$
 $N_{\text{H}} = 3.20 \cdot 10^{22} \text{ cm}^{-2}$ (fixed; Becker et al. 2002)

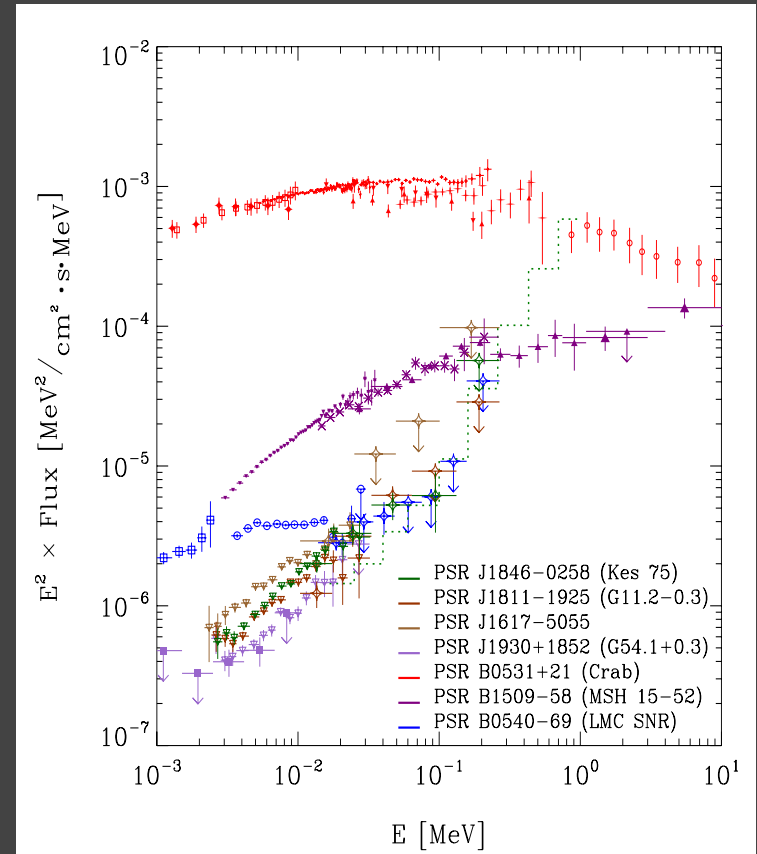
New Sample of Four young (< 10 ky) energetic pulsars emitting soft γ -rays

- “Old”: PSR B0531+21 (Crab), PSR B0540-69 and PSR B1509-58
- “New”: PSR J1846-0258, PSR J1930+1852, PSR J1811-1925, PSR J1617-5055
- Pulse profiles of new sample are similar to PSR B1509-58:
asymmetric single broad pulse



New Sample of Four young (< 10 ky) energetic pulsars emitting soft γ -rays

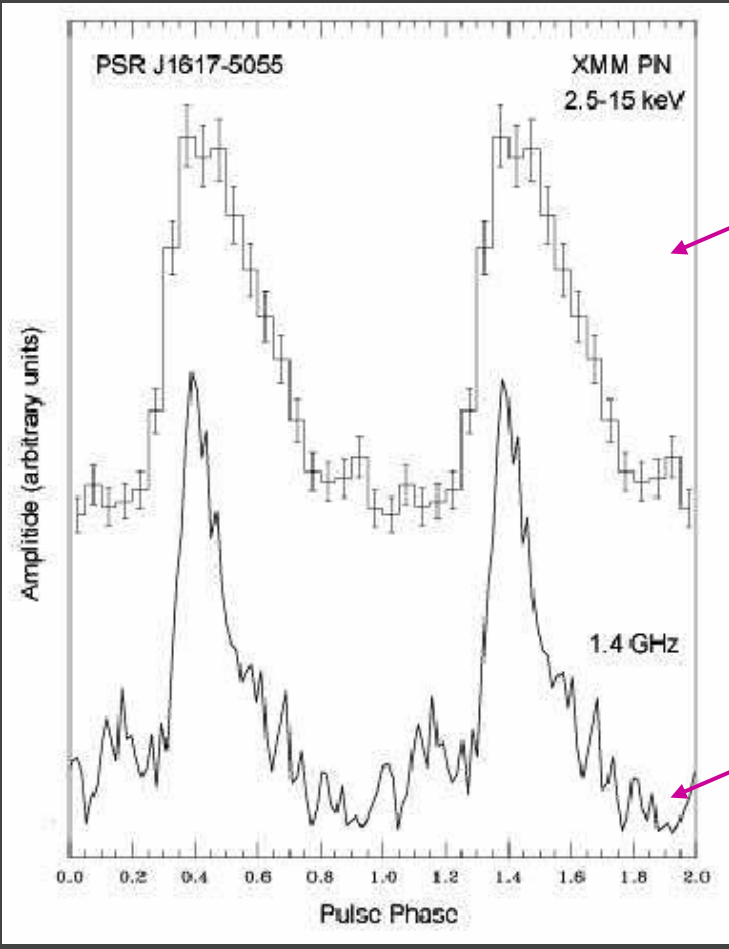
- “Old”: PSR B0531+21 (Crab), PSR B0540-69 and PSR B1509-58
- “New”: PSR J1846-0258, PSR J1930+1852, PSR J1811-1925, PSR J1617-5055
- Pulse profiles of new sample are similar to PSR B1509-58: asymmetric single broad pulse
- The hard X-ray/soft γ -ray spectral shapes of this sample pulsars are similar to the spectral shape of PSR B1509-58



Profiles of Young/Short-Period Pulsars

PSR B0540-69
50 ms pulsar in LMC

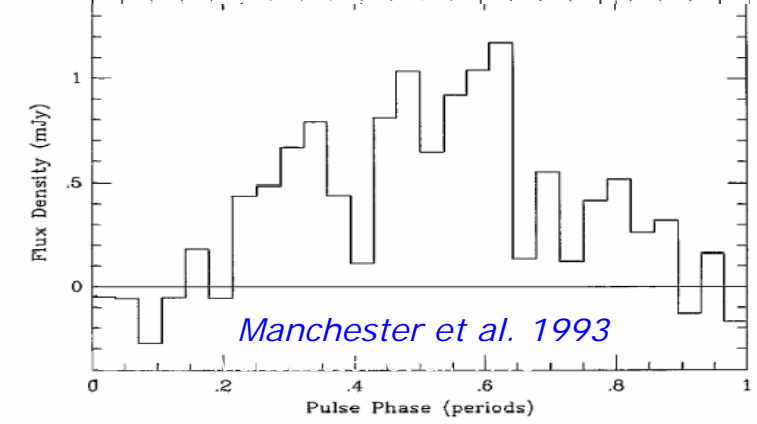
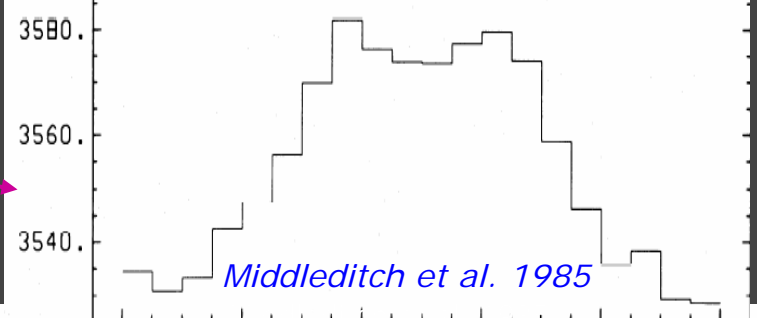
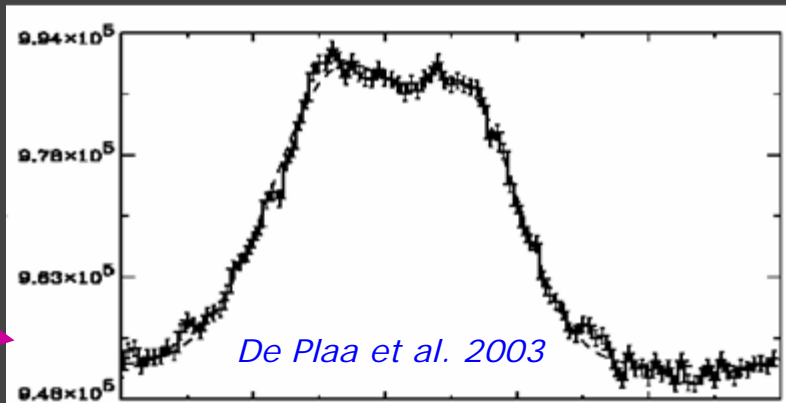
PSR J1617-5055
69 ms pulsar in RCW103



X-Ray

Optical

Radio



Spin-down Powered millisec Pulsars:

- Old, low B pulsars
- 7 systems show pulsed X-ray emission
- 2 sub-classes:

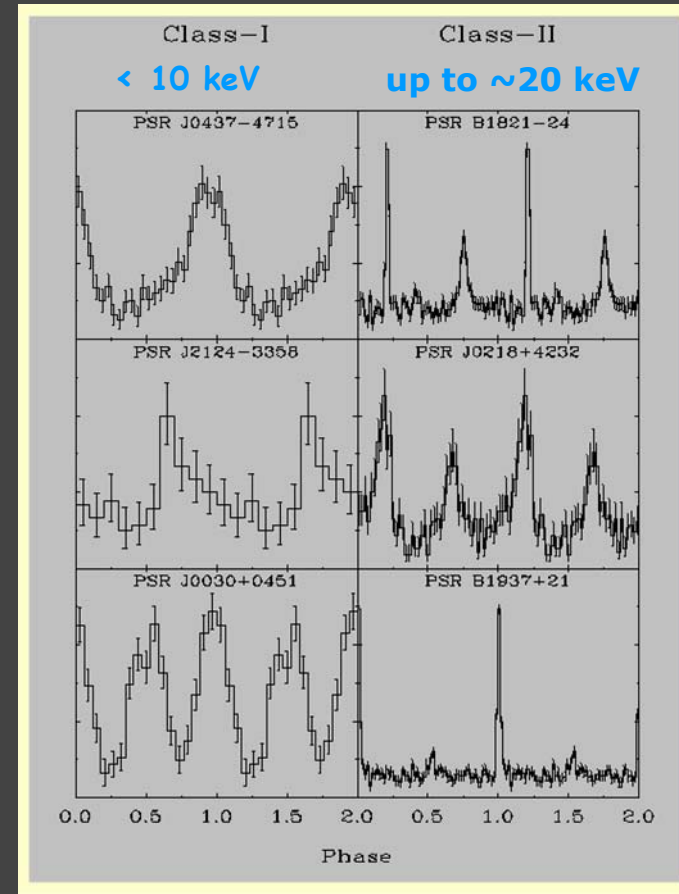
I - 4 have broad pulses
soft spectra

low luminosity (pulsed $\sim 10^{30}$ erg s $^{-1}$)
(seen because "nearby")

II - 3 have narrow pulses

hard spectra up to ~ 20 keV

high luminosity (pulsed $\sim 10^{32}$ erg s $^{-1}$)

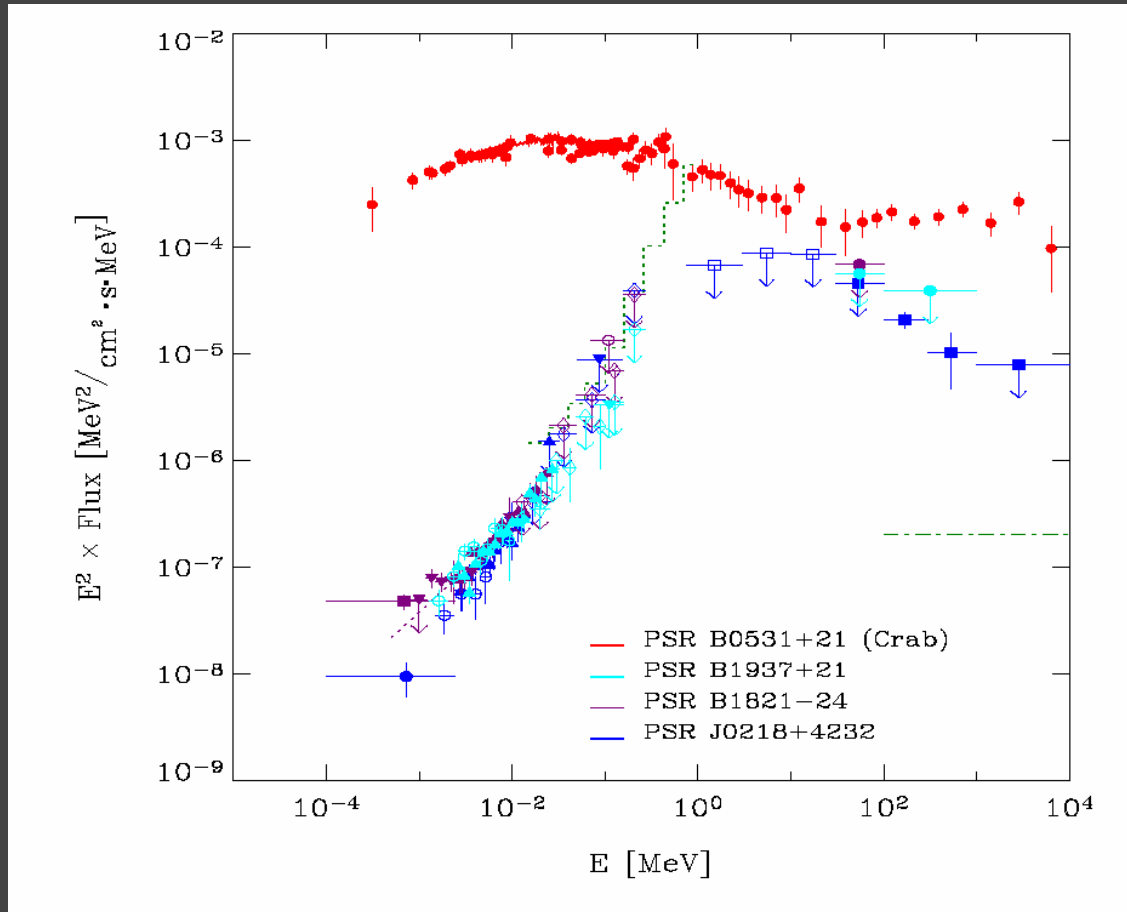


+ PSR J2124-3358
Zavlin 2005

Spin-down Powered millisec Pulsars, Class II

High-energy spectra

Kuiper & Hermsen 2003



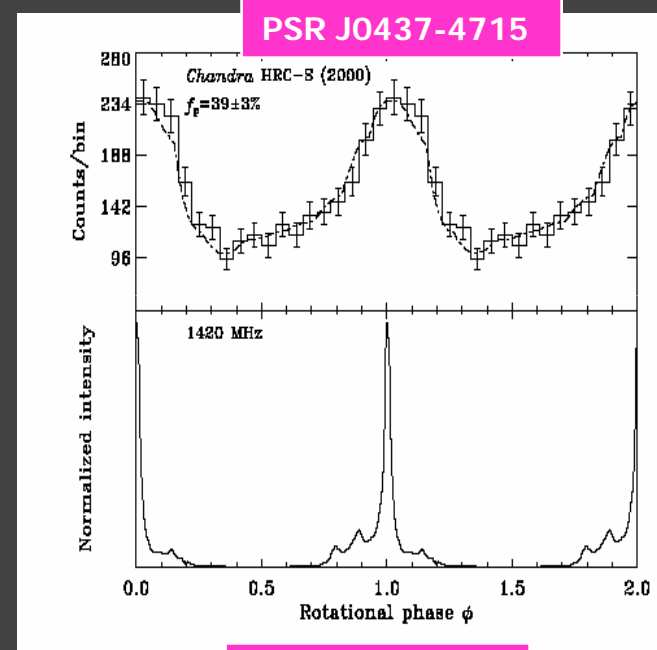
X-ray Photon spectral indices ~ 1.0

PSR 0218+4232 seen by EGRET up to 1GeV!

Profiles of millisecond pulsars

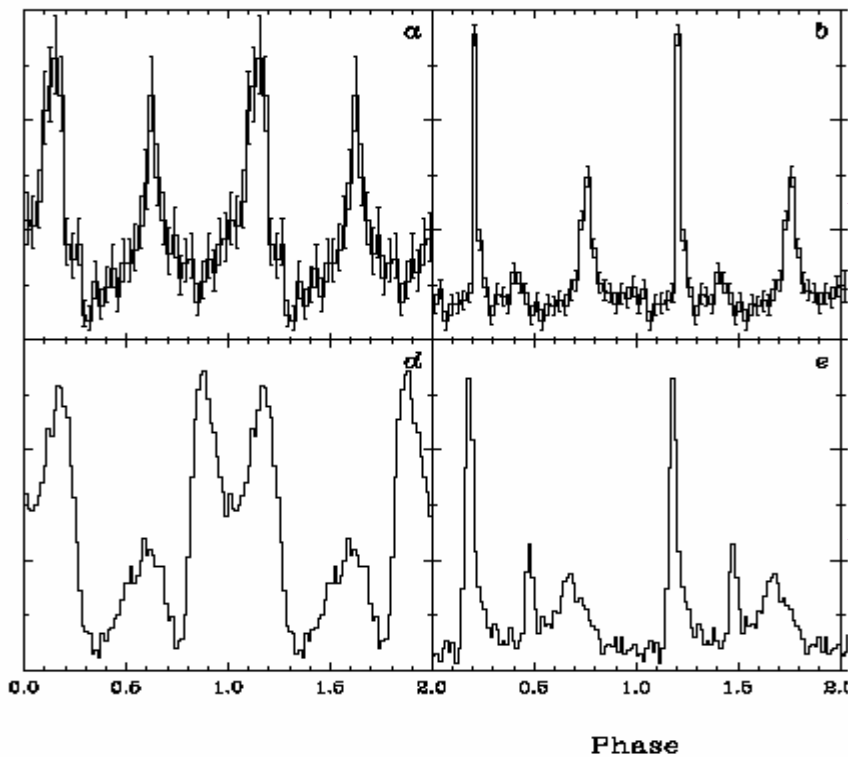
X-ray peaks (mostly) in phase with radio peaks

(Similar to Crab)



PSR J0218+4232

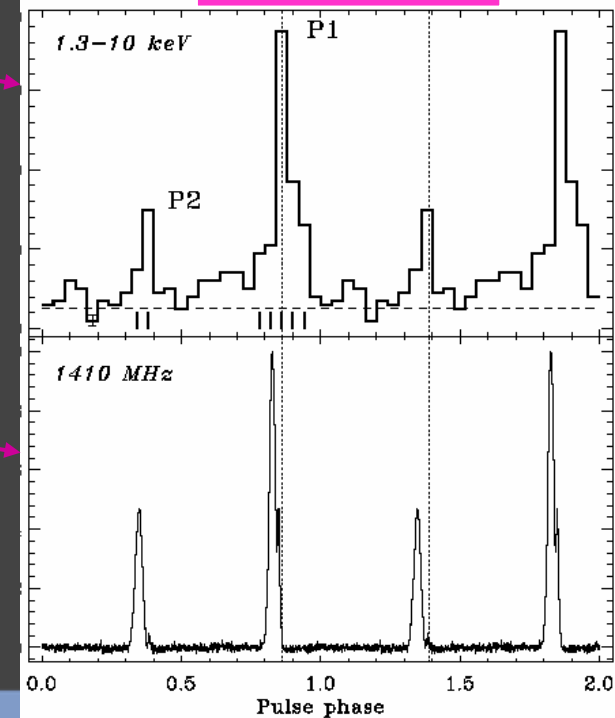
PSR B1821-24



X-Ray

Radio

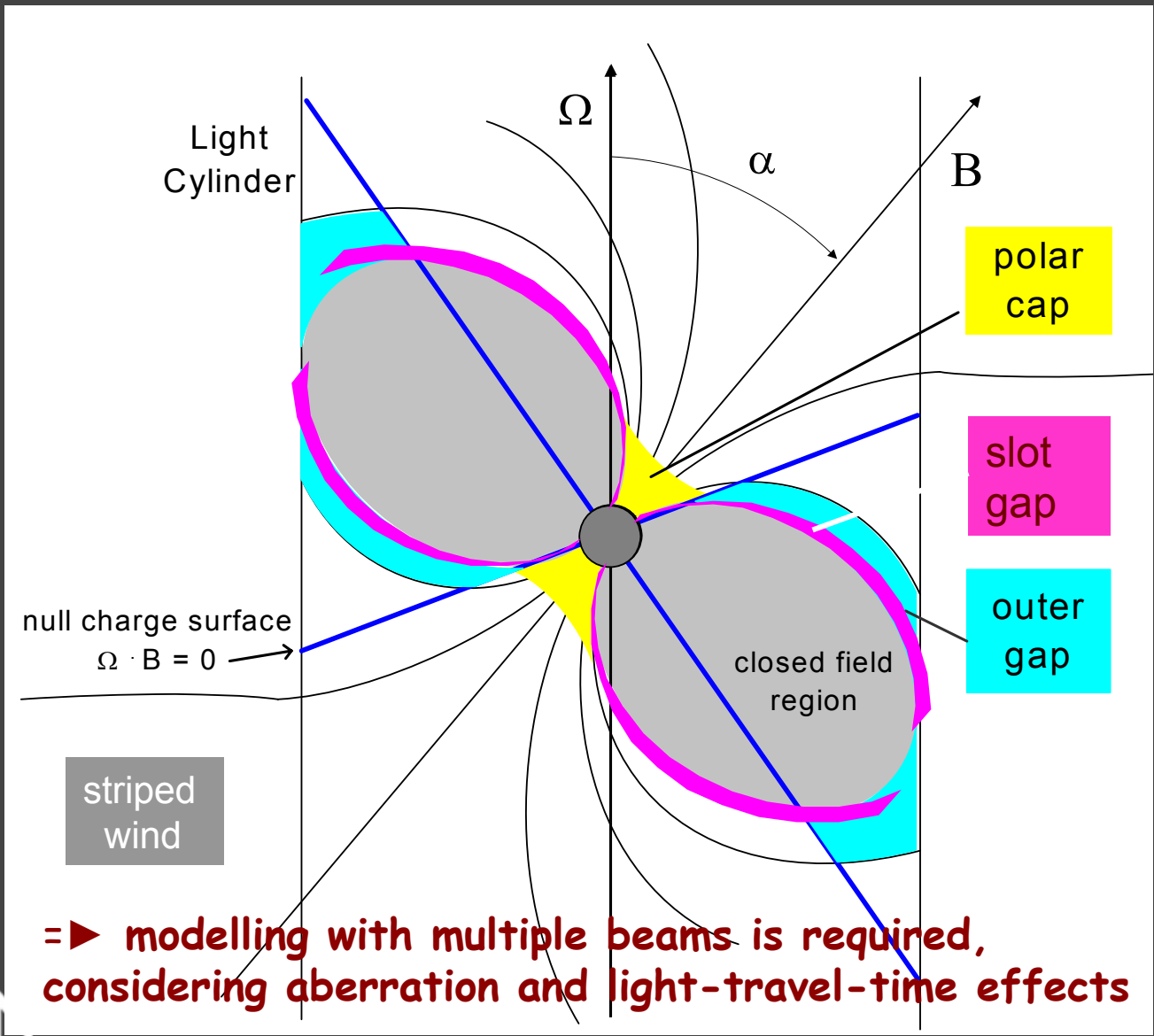
PSR B1937+21



Rotation-Powered Pulsars

- Review Emission Models, Comparison with Observations

Geometries of high-energy emission pulsar models



Rotating Magnetized Neutron stars I

- Unipolar inductors generating huge electric fields in vacuum: $\mathbf{E} = -(\boldsymbol{\Omega} \wedge \mathbf{r}) \wedge \mathbf{B}$
- However, a rotating neutron star will not be in vacuum, building up a large surface charge
- The \mathbf{E} -field component parallel to magnetic field, $\mathbf{E}_{//}$, can pull charge from crust against gravity creating a charge density in the magnetosphere known as the Goldreich-Julian or corotation charge density $\rho_{\text{GJ}} = -2 \epsilon_0 \boldsymbol{\Omega} \cdot \mathbf{B}$. (Goldreich & Julian 1969)
- When ρ_{GJ} is reached everywhere in magnetosphere, it will short out $\mathbf{E}_{//}$ and the dipole magnetic field will corotate with the star
- Corotation must break down at large distances from the neutron star due to particle inertia, certainly at the speed-of-light radius, R_c .
- The pulsed emission is presumed to originate inside the corotating magnetosphere, and strong $\mathbf{E}_{//}$ (**stable!**) may develop to accelerate particles at two possible sites where $\mathbf{E} \bullet \mathbf{B} \neq 0$ and $\rho < \rho_{\text{GJ}}$:
 - 1) Near magnetic poles in inner magnetosphere – polar-cap models
 - 2) In outer magnetosphere along last closed field lines – outer-gap models
- Primary charges can be accelerated in this $\mathbf{E}_{//}$, along the magnetic field lines to energies as high as ~ 10 TeV, and will emit photons

Rotating Magnetized Neutron stars II

- Incoherent processes produce optical, X-ray and gamma-ray photons:
curvature and synchrotron radiation, Compton upscattering
(fraction $\sim 10^{-3}$ to 10^{-1} of $E_{\text{spin down}}$)
- Coherent processes responsible for radio emission
(tiny fraction $\sim 10^{-6}$ of $E_{\text{spin down}}$)

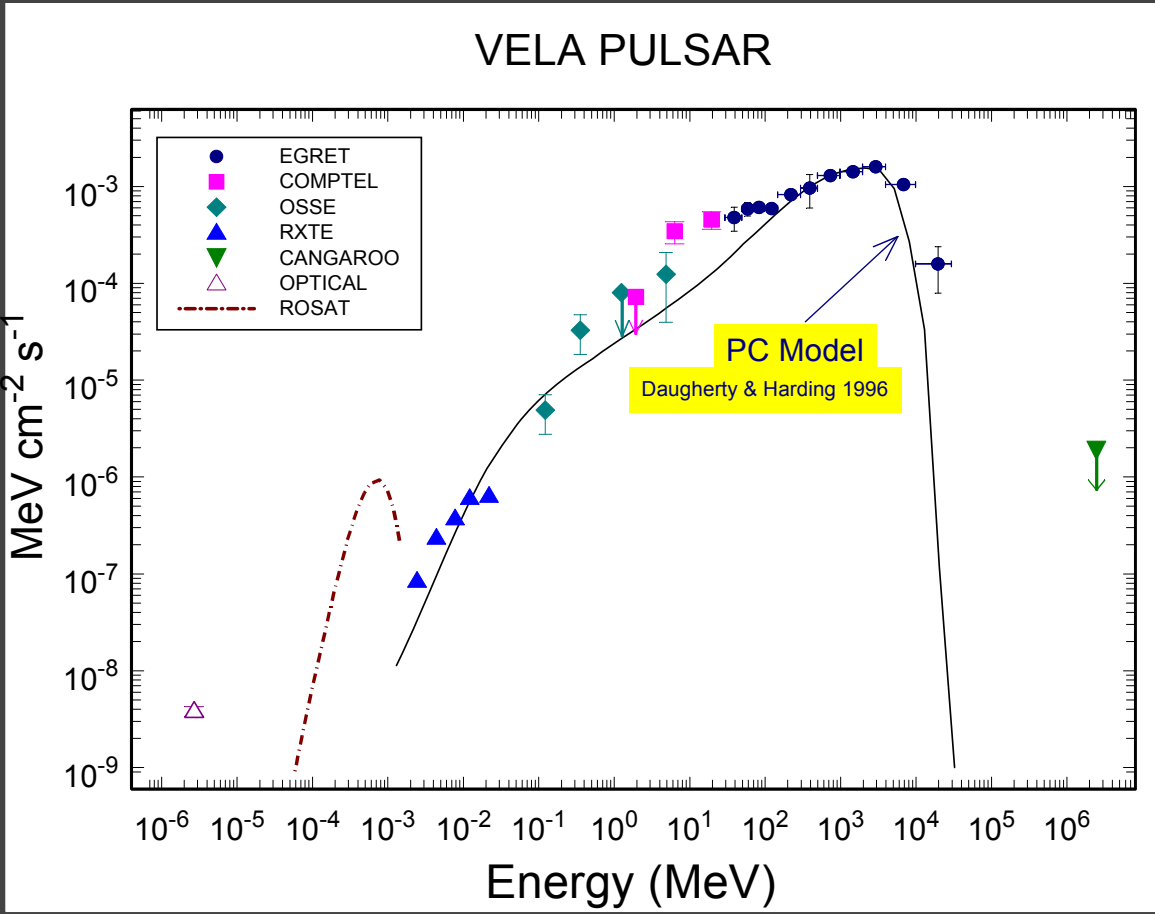
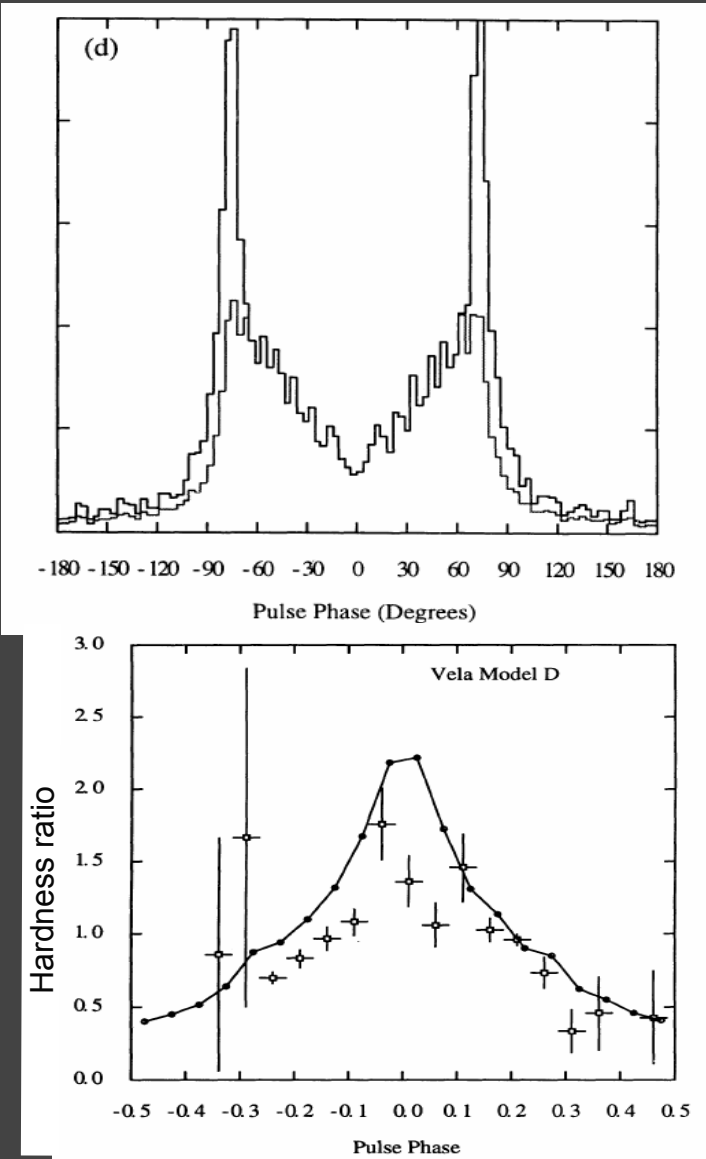
Polar Cap Model

Harding et al. 1978, Daugherty & Harding 1982 & 1996 , Usov & Melrose 1995

- Voltage develops along open field lines near and above polar cap surface
- Particle acceleration occurs near the neutron star surface
- High-energy emission results from a curvature-radiation or inverse-Compton induced pair cascade in the strong field
- The induced pairs can radiate synchrotron photon → more pairs
- Two subclasses:
 - a) **Vacuum gap models**: particles trapped in ns surface layers and a vacuum gap forms above surface
 - b) **Space-Charge Limited Models**, in which charges are freely emitted from the surface and a voltage develops due to the small charge deficit between ρ and ρ_{GJ}

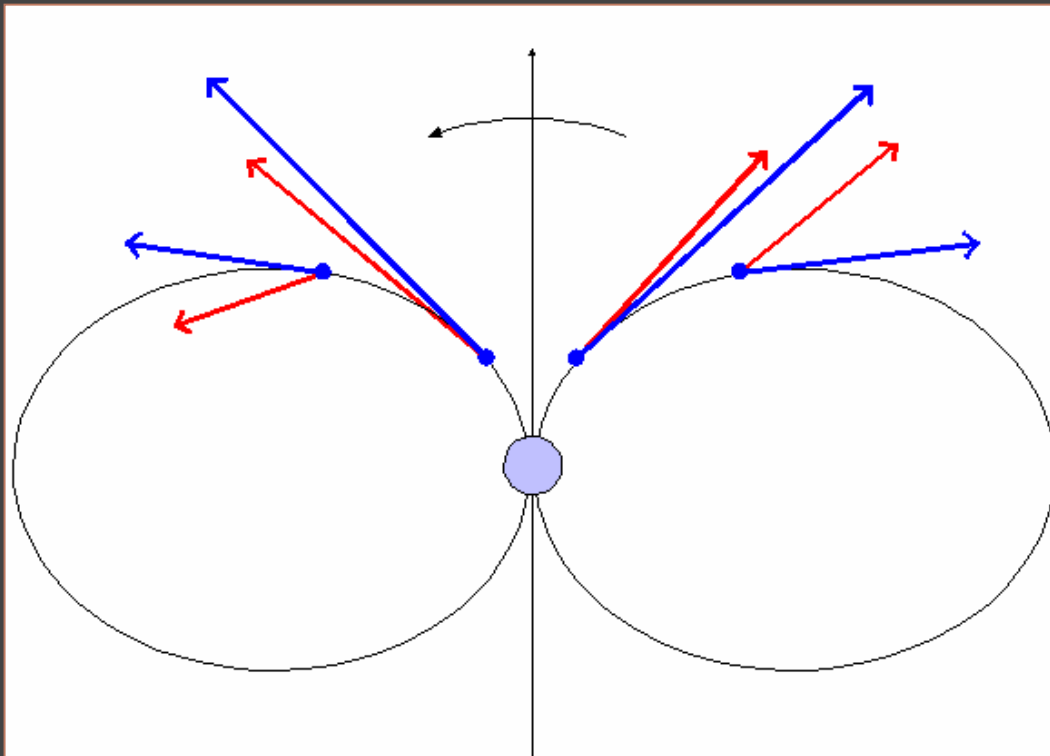
Traditional PC Model (Daugherty & Harding 1996)

- Acceleration artificially placed at $r = 3 R$
- Assumed PC rim enhancement
- $\alpha = 10^0$ to generate broad pulse profile

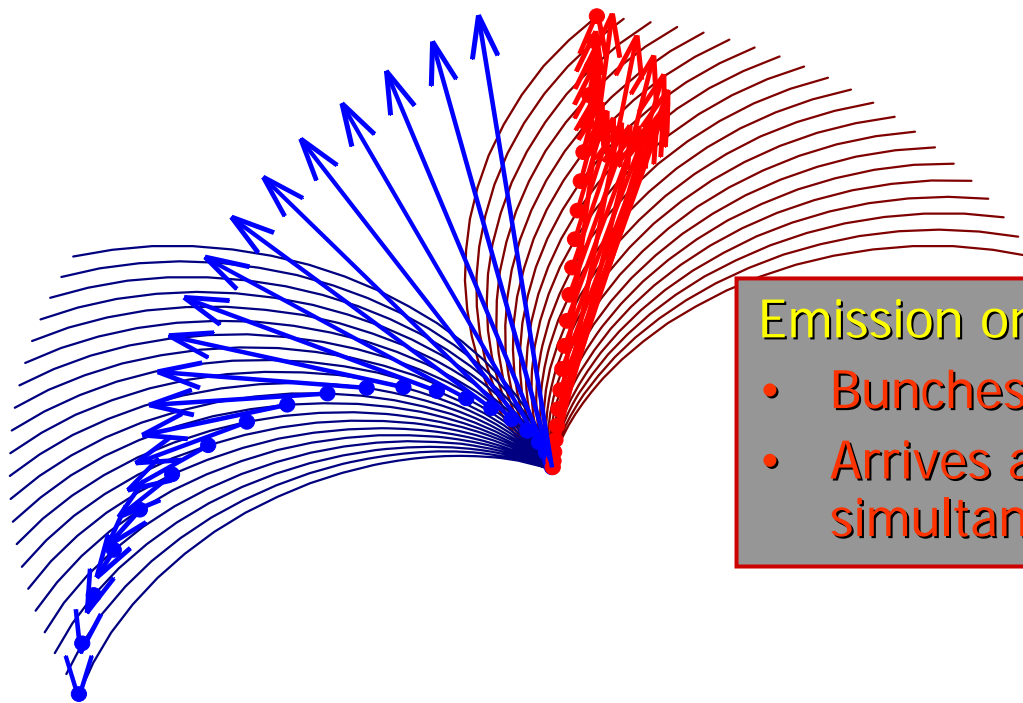


Caustic emission (Morini 1983)

- Particles radiate along last open field line from polar cap to light cylinder
- Time-of-flight, aberration and phase delay cancel on trailing edge \longrightarrow emission from many altitudes arrive in phase \longrightarrow **caustic** peaks in light curve



Formation of caustics



Emission on trailing field lines

- Bunches in phase
- Arrives at inertial observer simultaneously

Emission on leading field lines

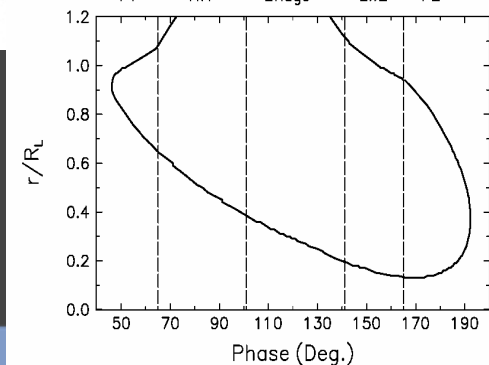
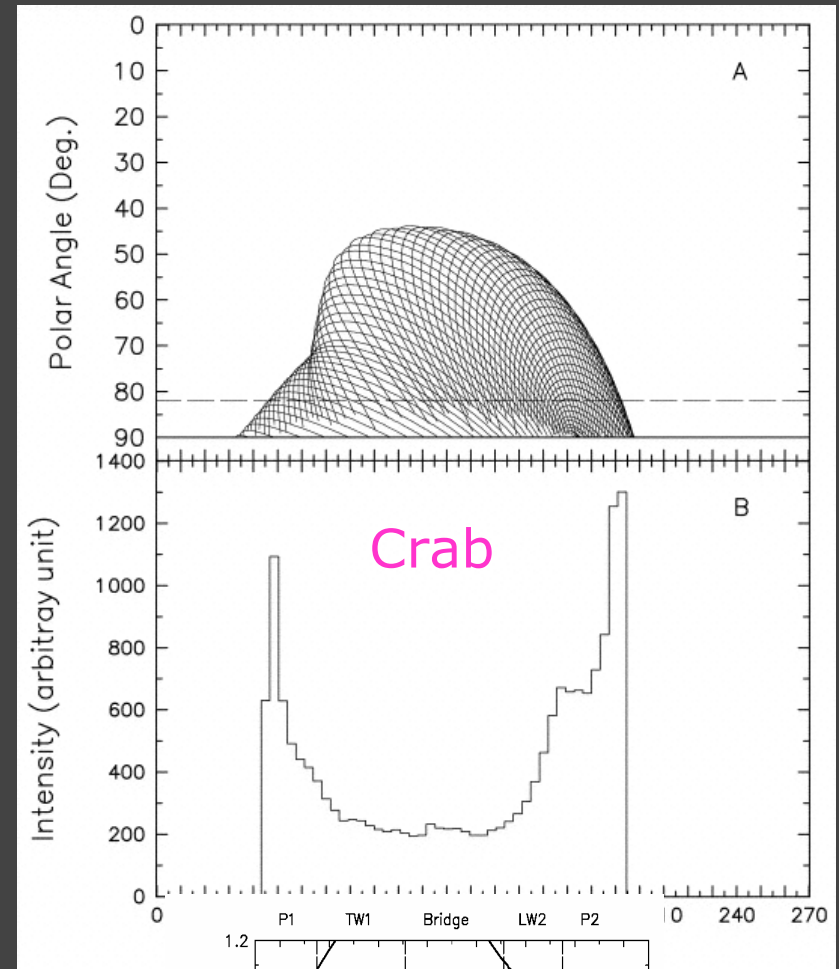
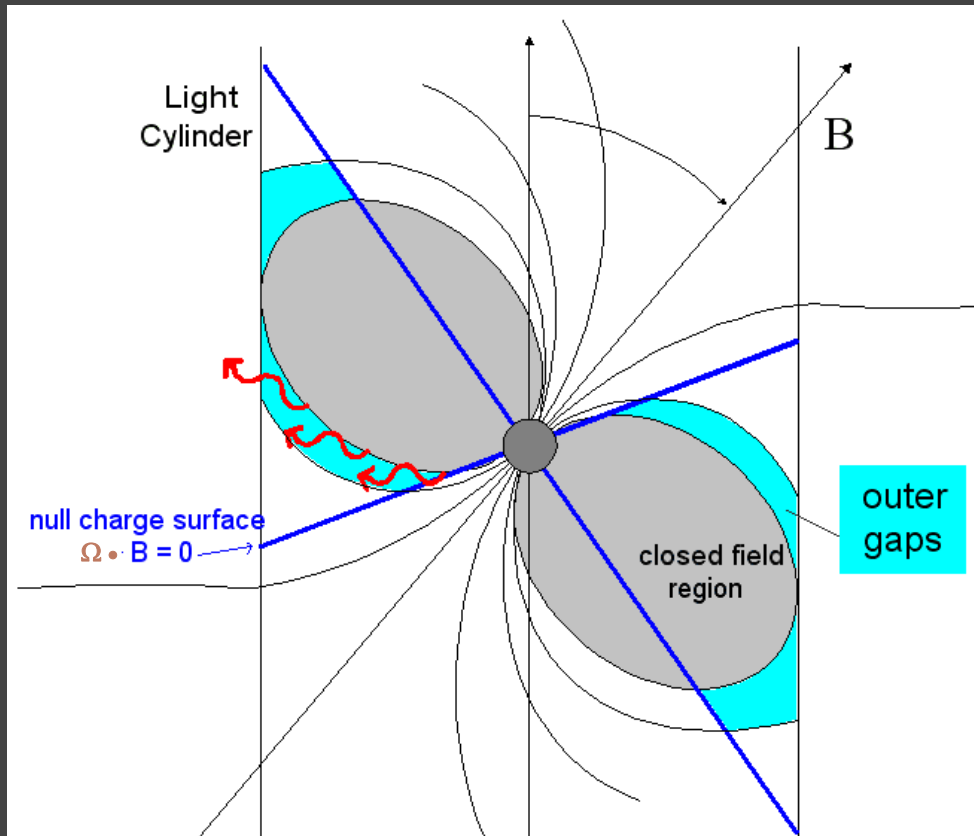
- Arrives at inertial observer at different times
- Spreads out in phase

Caustic emission

- Dipole magnetic field
- Outer edge of open volume

Outer Gap Model

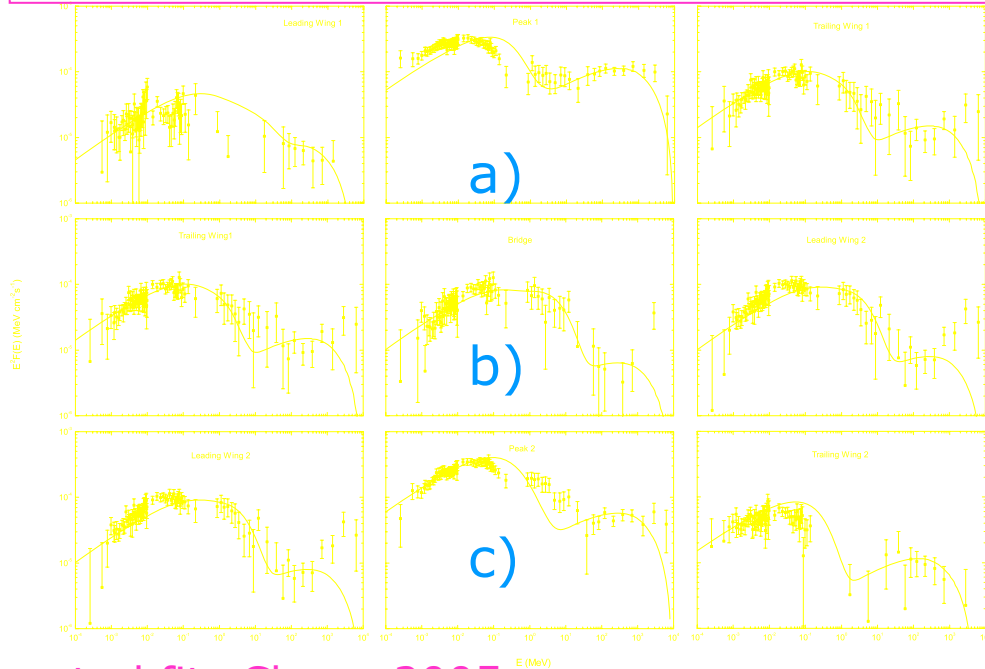
Romani & Yadigaroglu 1995
Cheng, Ruderman & Zhang 2000



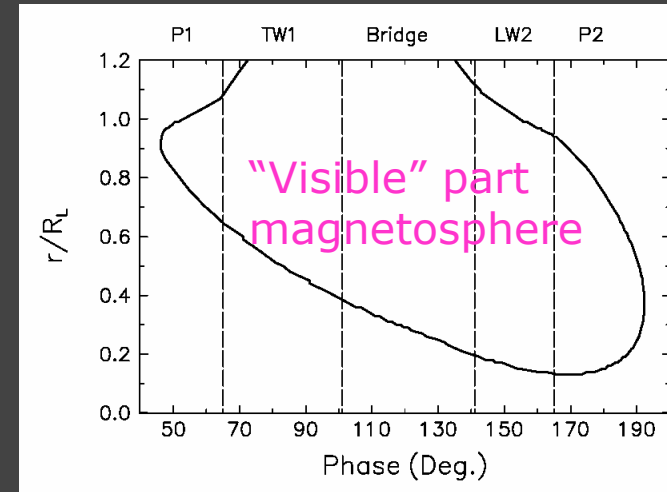
No "off pulse"/tail emission in modelled profile

Outer Gap Model (Cheng, Ruderman & Zhang 2000)

Crab phase-resolved spectra, Kuiper et al. 2000



Spectral fits Cheng 2005

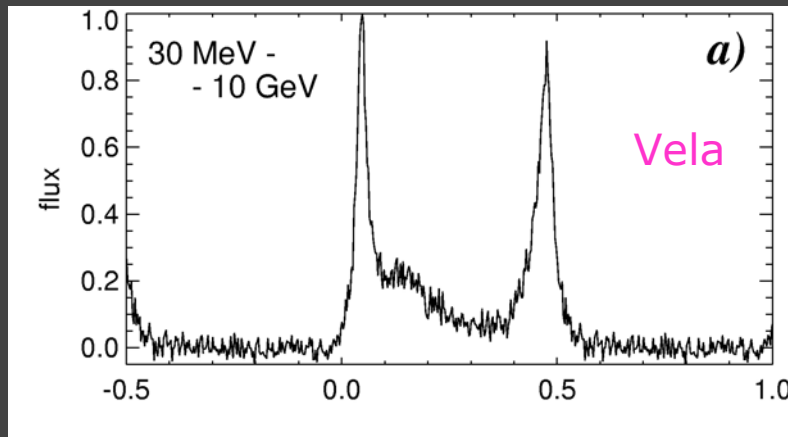


- a) 1st Peak emission dominated by curvature radiation
- b) Bridge emission by synchrotron radiation
- c) 2nd Peak curvature plus synchrotron radiation

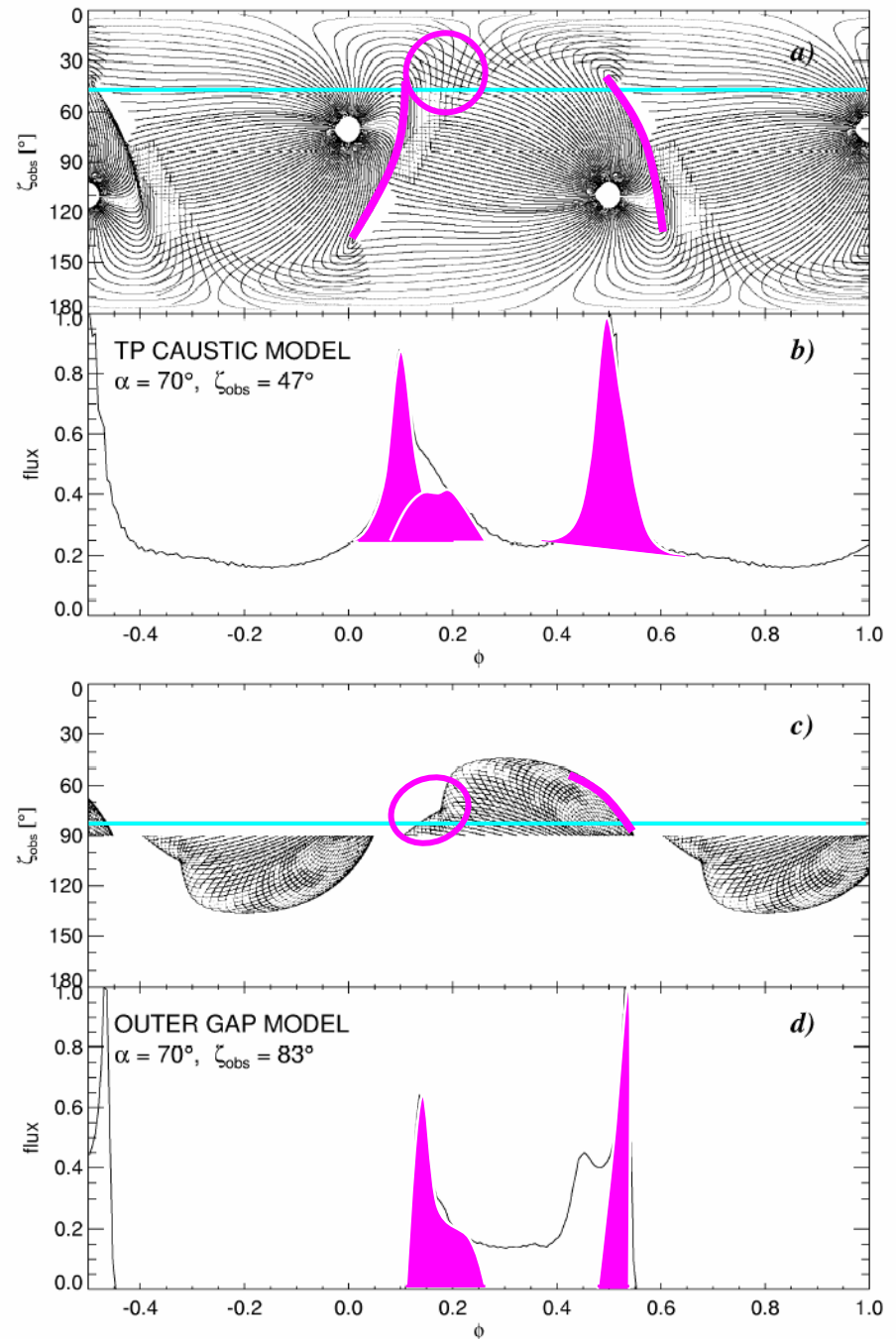
Two-pole caustic and outer gap models

Dyks & Rudak 2003

Dyks, Harding & Rudak 2004

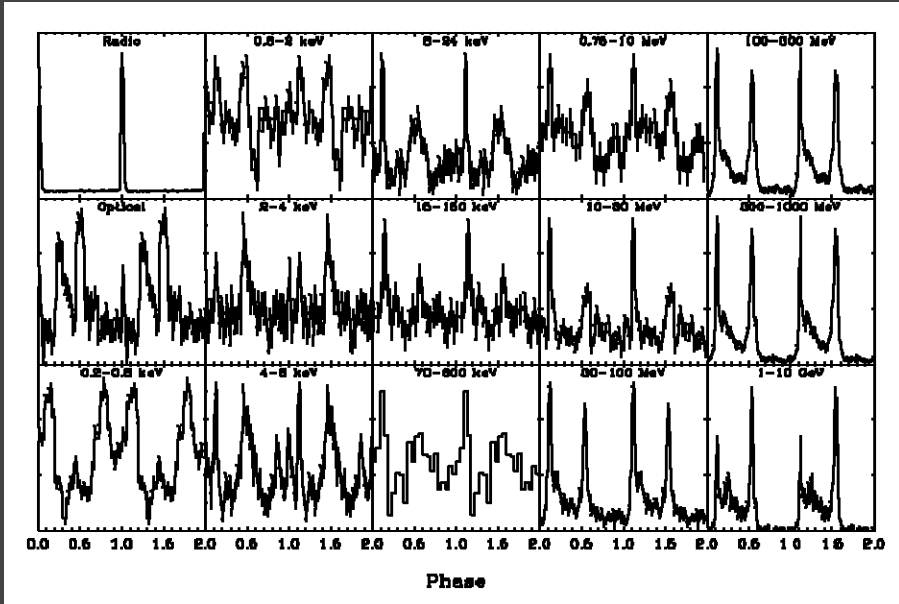


- TPC reproduces better the Vela profile than the OG model
- For TPC emission over all phases

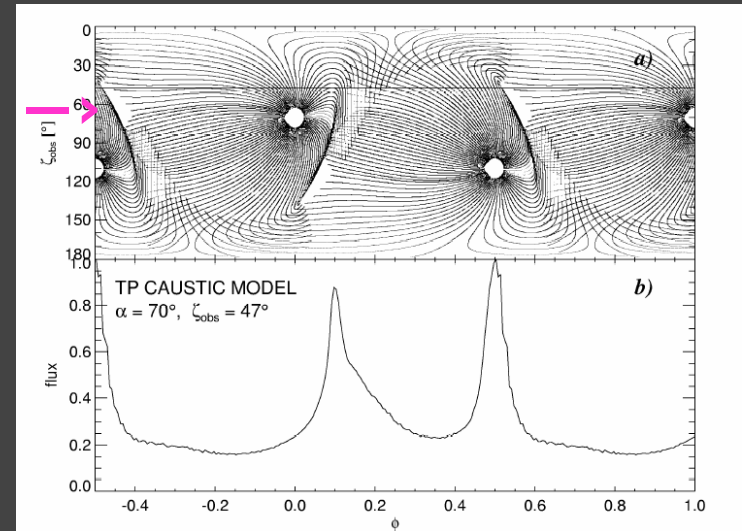


Two-pole caustic model

Vela multiwavelength profiles



TPC Dyks, Harding & Rudak 2004

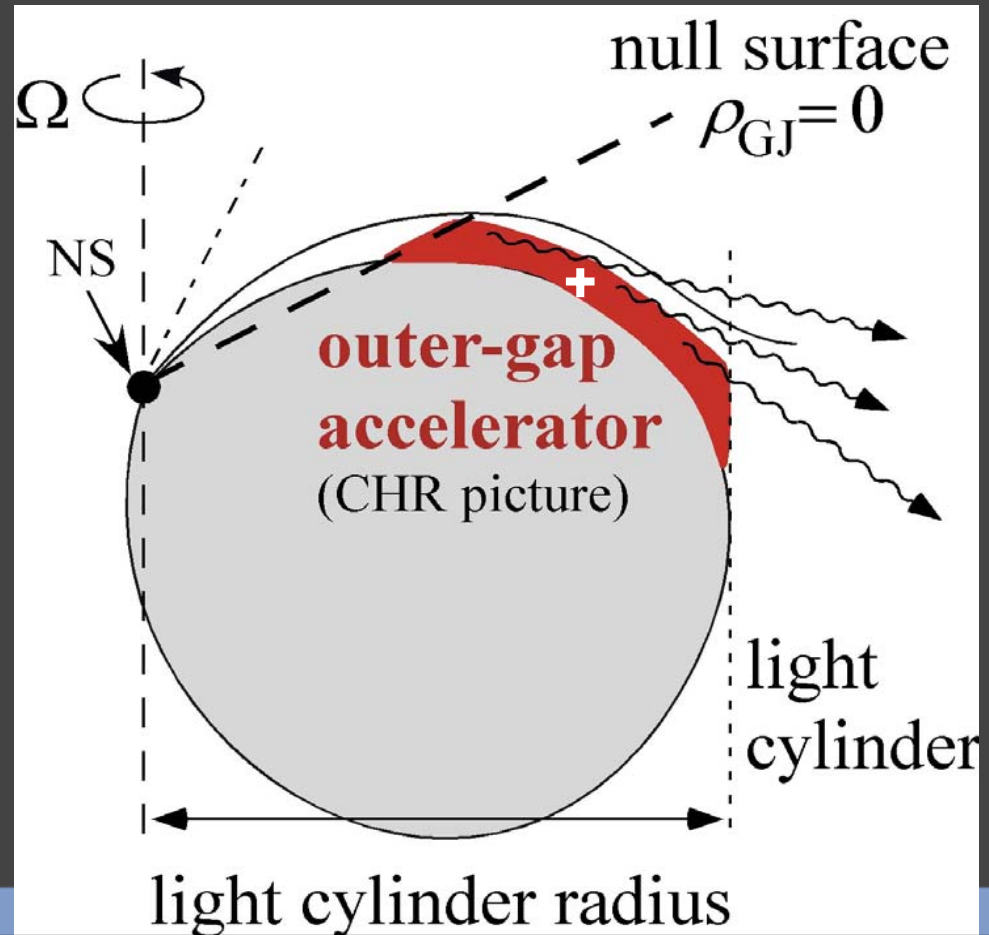


- TPC model can produce additional narrow pulses, e.g. for slightly different viewing angles the polar cap region becomes visible
- However, TPC has difficulties in producing single broad pulses, e.g. like seen now for several young pulsars

Extended Outer Gap Model

Hirovani, Harding, Shibata 2003

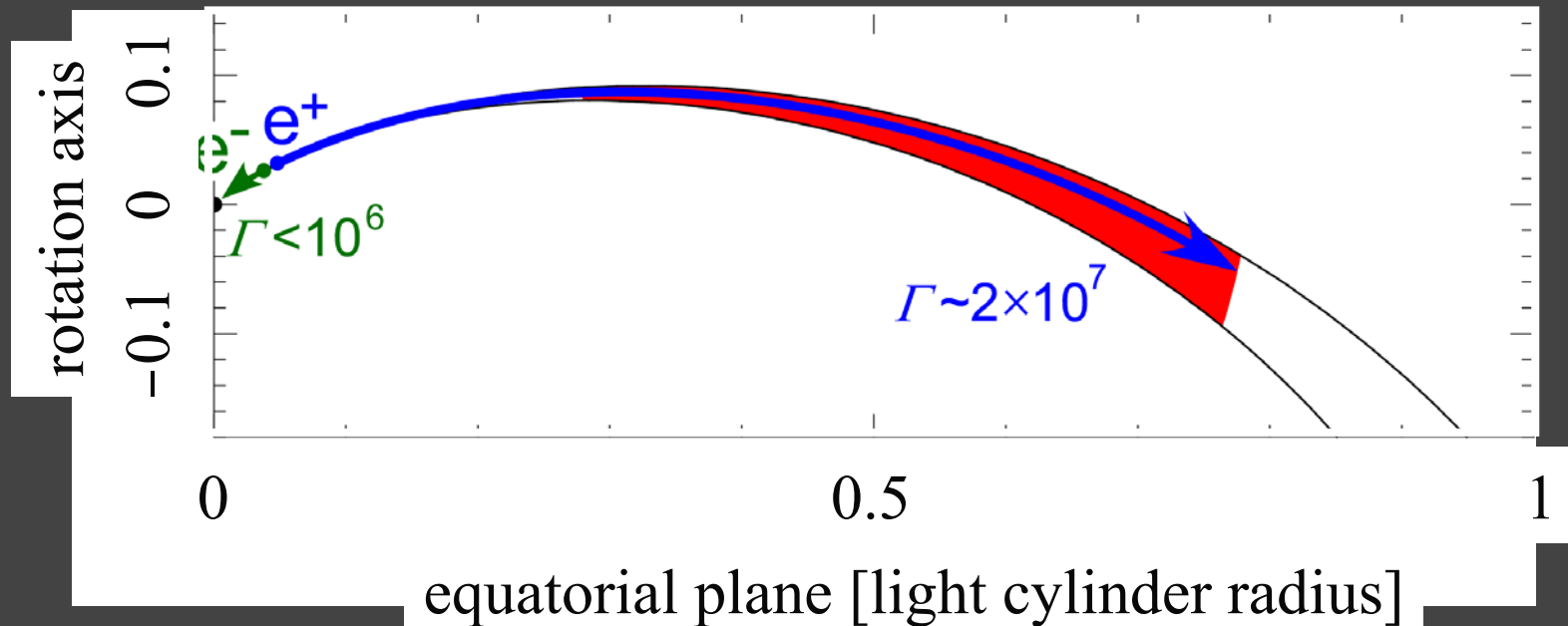
- The hypothesized gap geometry does not satisfy the Maxwell equation
- They solved the set of **Maxwell & Boltzmann equations** in pulsar magnetospheres on 2-D poloidal plane
- Found that the gap extends from the vicinity of the N.S. to the outer magnetosphere



Extended Outer Gap Model

Hirovani, Harding, Shibata 2003

- Resulting geometry is getting closer to that of the two-pole caustic model (TPC)
- This extended outer gap might also offer a physical explanation for the TPC



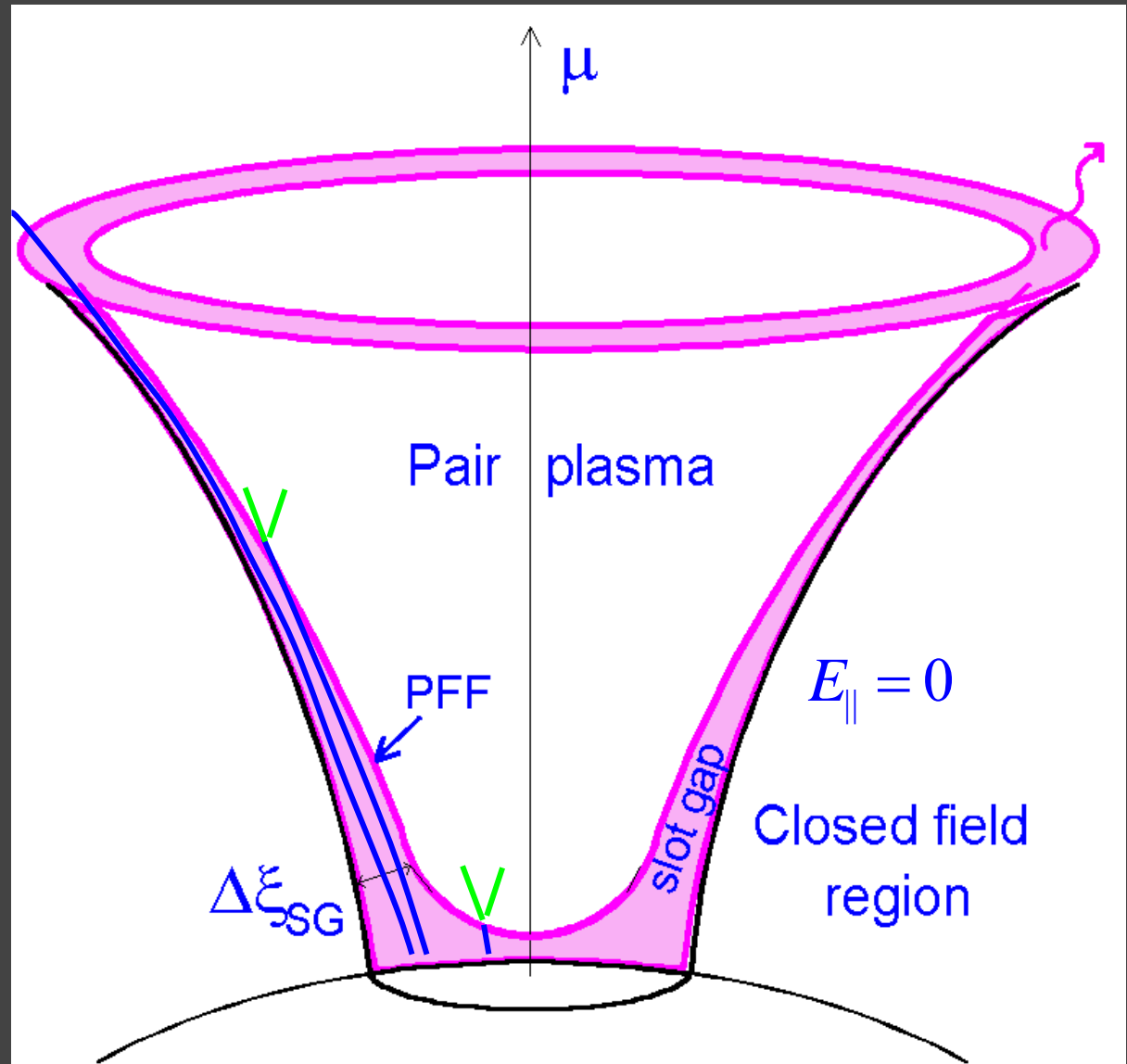
Slot gap model, physical justification for TPC

- Pair-free zone near last open field-line

(Arons 1983, Muslimov & Harding 2003, 2004)

- Slower acceleration
- Pair formation front at higher altitude
- Slot gap forms between conducting walls

- E_{\parallel} acceleration is not screened



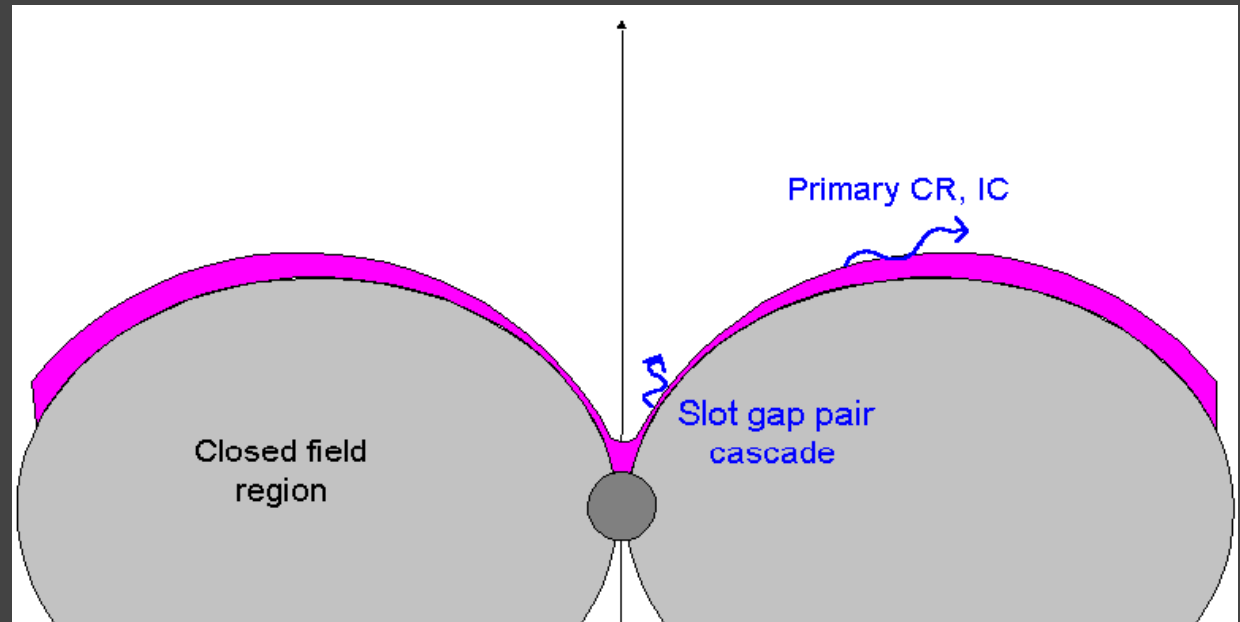
Slot gap model, physical justification for TPC

- Pair-free zone near last open field-line

(Arons 1983, Muslimov & Harding 2003, 2004)

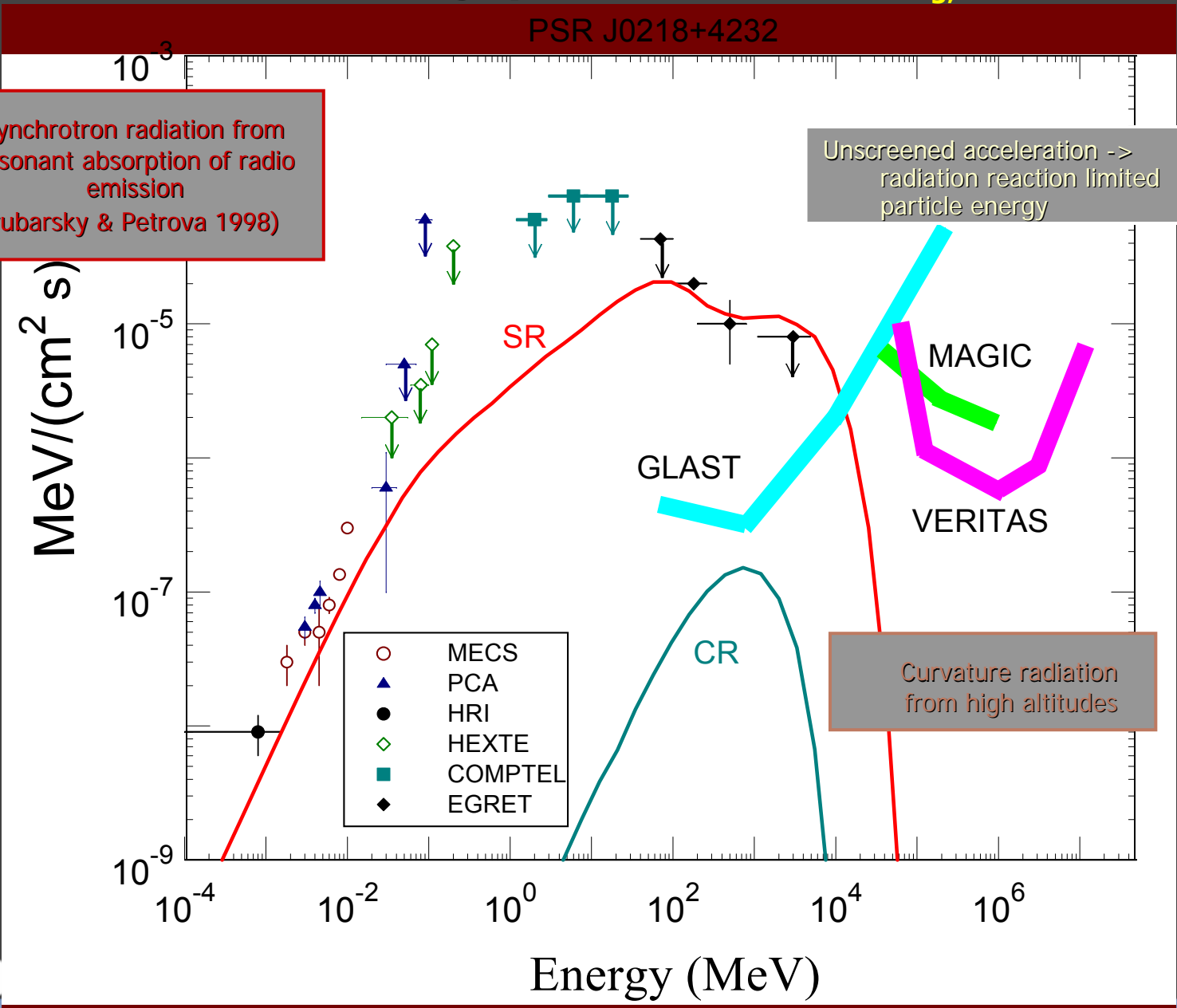
- Slower acceleration
- Pair formation front at higher altitude
- Slot gap forms between conducting walls

- $E_{||}$ acceleration is not screened

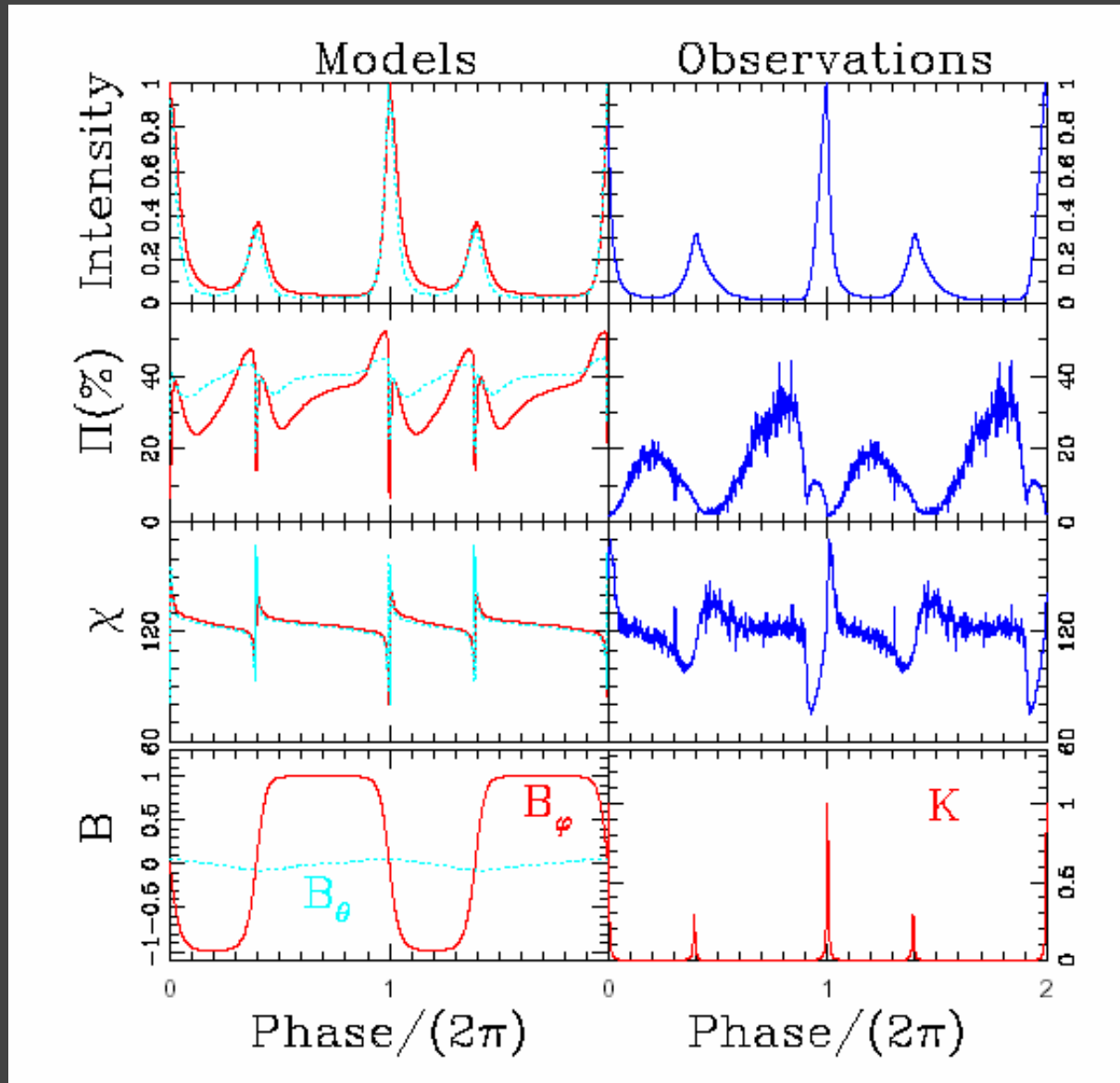


The strange spectrum of ms-pulsar J0218+4232 modelled with slot gap model

Harding, Usov & Muslimov 2005



Emission from a striped wind, production beyond the light cylinder radius See: Petri & Kirk 2005



Observing Rotation-powered Pulsars in the X-ray and Gamma-Ray Sky

Challenges, open questions:

- Theory: There is no consistent model yet that can satisfactorily explain the available data.
- Observations: There are still only two pulsars which have been measured over the total X-ray / gamma-ray range:
Crab and Vela!

There are / will be many opportunities for new observations:
XMM-Newton, Chandra, Suzaku, RXTE, INTEGRAL, Swift, AGILE,
GLAST, HESS, MAGIC, VERITAS,

**==> Given the sensitivity of current and planned missions,
between 20 keV and 100 MeV very long observations will
remain required to make progress**